Biocontrol against fungal mycoparasites driven by *Bacillus velezensis* strains from a mushroom crop microcosm

William Kay[‡,1]; Jaime Carrasco[‡,1,2,3,4*], Souvik Kusari[5,6], Marjon Krijger[7]; M. José Carpio[4,8], Thomas Barnes[1]; M. Sonia Rodríguez Cruz[4,] Jan van der Wolf[7]; Till Bebenroth[6]; and Gail Preston*[1]

[‡]These authors are joint first authors

[1]Department of Biology, University of Oxford, South Parks Road, Oxford OX1 3RB, UK.

[2]IRIAF – Agri-food and Forestry Regional Research and Development Centre, CIAF - Agroforestry Research Centre, Carretera Toledo-Cuenca km 174, Cuenca 16194, Spain.

[3]Centro Tecnológico de Investigación del Champiñón de La Rioja (CTICH), Autol, Spain.

[4]Institute of Natural Resources and Agrobiology of Salamanca, IRNASA-CSIC, Cordel de Merinas 40-52, 37008 Salamanca, Spain.

[5]Department of Genetics, Institute of Biology and Ecology, Faculty of Science, Pavol Jozef Šafárik University in Košice, Mánesova 23, 04154 Košice, Slovakia.

[6]Center for Mass Spectrometry, Faculty of Chemistry and Chemical Biology, Technische Universität Dortmund, 44227 Dortmund, Germany.

[7]Wageningen University and Research, Biointeractions & Plant Health, 6700 AA Wageningen, the Netherlands;

[8]Institute of Agricultural Sciences, ICA-CSIC, Serrano 115 bis, 28006 Madrid, Spain

20 *Corresponding authors: jcarrasco@jccm.es (JC); gail.preston@biology.ox.ac.uk (GP)

21 **Keywords:** *Agaricus bisporus*; Mycoparasites, Casing material; Biocontrol; Secondary
22 metabolites, Specialised metabolites, Lipopeptides.

23 **Abbreviations:** NGS, next generation sequencing; CD, cobweb disease; DBD, dry bubble
24 disease; WBD, wet bubble disease; PLFA, phospholipid fatty acid.

25 **Repositories:** Sequence data for this study are deposited in NCBI BioProject collection under
26 BioProject ID PRJNA1142391.

27 Abstract

28 The cultivation of button mushroom (*Agaricus bisporus*) requires the design of tailor-made
29 substrates that nourish the crop and promote morphology changes from mycelium to
30 basidiome. The agronomic stages of mushroom development are also influenced by the
31 microbiota present in the mushroom crop microcosm, which may have a beneficial impact on
32 mushroom growth, development and quality, or a detrimental impact through reduction of yield
33 or quality as pathogens, competitors or disease vectors in mushroom crops. *Bacillus velezensis*
34 strains isolated from commercial mushroom casing material have been demonstrated to have
35 antifungal activity against fungal mycoparasites of mushroom crops. In this report we describe
36 the isolation of multiple strains of *B. velezensis* from mushroom casing material and basidiomes
37 that show antifungal activity towards major mushroom mycoparasites, along with further
38 characterization of their mode of action. Full genomes of *B. velezensis* CM5, CM19, CM35,
39 EM5 and EM39 were sequenced and annotated, which together with metabolic profiling of
40 specialised metabolites produced by CM5, CM19 and CM35 suggested that antifungal activity
41 of these strains is linked to the production of the lipopeptide fengycin. However, in crop trials,

these strains did not increase mushroom yield or provide significant control of the mushroom pathogen *Lecanicillum fungicola.* Genomic and analytical tools were designed and used to evaluate *B. velezensis* persistence in casing when the selected strains were artificially applied. *B. velenzensis* population levels decreased significantly after application, potentially contributing to the lack of biocontrol activity observed in crop trials.

Introduction

The commercial cultivation of the secondary decomposer white button mushroom (*Agaricus bisporus*) is based on the transformation of agricultural and farming by-products into selective nutritional substrates by means of a 3-phase composting strategy: i) maturation of raw materials through subsequent mesophilic and thermophilic stages; ii) production of a parasite-free substrate through a pasteurization and stabilization stage; iii) induction of *A. bisporus* mycelium growth in the selective compost (Wang *et al.*, 2021). When the selective substrate is fully colonized by the mycelium it is placed in environmentally controlled growing units and topped with bio-based casing material to provide the physical, chemical and microbiological requirements to induce basidiome fructification(Dias *et al.*, 2021).

Microbial parasites are a major issue for crop losses in the food industry (Fones *et al.*, 2020). The fungal parasites associated with green mould (*Trichoderma* spp.), wet bubble (*Mycogone perniciosa*), dry bubble (*Lecanicillium fungicola*), and cobweb (*Cladobotryum spp.*) are responsible for the majority of reported losses caused by pathogenic or competing fungi within the mushroom industry (Gea *et al.*, 2021). It is worth mentioning the difficulty of breeding for resistance in *Agaricus bisporus*, which lies in the typical life cycle of this fungus, which hampers the introduction of traits without considerable linkage drag (Sonnenberg *et al.*, 2017). Therefore, to fight such harmful fungal mycoparasites, selective agricultural fungicides have

65 historically been used in mushroom farms, including chlorothalonil, carbendazim, metrafenone
66 or prochloraz-Mn (Kosanović et al., 2013; Commission E., 2019). However, these fungicides
67 are now either prohibited, or are no longer effective due to resistance outbreaks, necessitating
68 the development of alternative approaches for disease control. Together with efficient hygiene,
69 biocontrol is a potential strategy to replace chemical pesticides as part of integrated disease
70 management programmes (Gea *et al.*, 2021).

71 There are multiple mechanisms of biocontrol described depending on the agent employed,
72 including: antagonism though production of lytic enzymes, antimicrobial peptides,
73 antimicrobial volatile organic compounds (VOCs) or other antibiotics; spatial and nutritional
74 competition; stimulation of mushroom growth through mycohormone production; and
75 enhanced nutrient uptake to improve the fungal immune system (Zhang and Sun, 2018;
76 Carrasco and Preston, 2020).

77 *B. velezensis* is a bacterial species that includes several relatively well-studied strains with
78 biocontrol activity. These are reported to produce antimicrobial metabolites that are able to
79 control both bacteria and fungi (Rabbee *et al.*, 2023; Kenfaoui *et al.*, 2024). Examples of
80 antimicrobial metabolites produced by *B. velezensis* include bacillaene, bacillibactin, bacilysin,
81 difficidin, fengycin, macrolactin H and subtilin (Pandin *et al.*, 2018). Of these, fengycin - a
82 lipopeptide with strong antifungal activity - is of particular interest in attaining control over
83 fungal parasites of mushrooms. Fengycin (also known as plipastatin) is synthesized by a non-
84 ribosomal peptide synthetase (NRPS) complex encoded by a large gene cluster known as the
85 *fen* operon (*pps* in *B. subtilis*). This operon encodes five enzymes, each responsible for
86 recognizing and incorporating specific amino acids during the process of building the final
87 fengycin peptide (Zihalirwa Kulimushi *et al.*, 2017; Desmyttere *et al.*, 2019; Gao *et al*., 2019).
88 Fengycin is known to disrupt fungal cell membranes by interacting with sterols, leading to

89 increased membrane permeability and cell death (Mantil *et al.*, 2019). Fengycin, and biocontrol
90 agents which produce fengycin, have been shown to be active against many fungal parasites of
91 mushroom crops including *Trichoderma aggressivum* (Pandin *et al.*, 2019; Kosanović et al.,
92 2021), *Cladobotryum mycophilum* (Clarke *et al.*, 2022a; Clarke *et al.*, 2024), *Lecanicillium*
93 *fungicola* (Clarke *et al.*, 2022) and *Mycogone perniciosa* (Novikova and Titova, 2023).

94 There are multiple classes of fengycin broadly classified into two main classes. These are
95 categorised using the amino acid present at the sixth position of the protein chain, with fengycin
96 A containing alanine, and fengycin B containing valine (Steller *et al.*, 1999). Further classes of
97 fengycins produced by *Bacillus* strains have also been described (Yin *et al.*, 2024), including
98 for instance fengycin S and fengycin C produced by *Bacillus amyloliquefaciens* LSC04 and
99 *Bacillus subtilis* EA-CB0015, respectively (Lee *et al.*, 2010; Villegas-Escobar *et al.*, 2013). In
100 *B. amyloliquefaciens* the production of these lipopeptide analogues has been shown to be
101 subject to positive regulation by the quorum sensing system encoded by the *comQXPA* gene
102 cluster (Yin *et al.*, 2024). The ComQXPA system is not unique to *B. amyloliquefaciens* or *B.*
103 *subtilis* (Kalamara *et al.*, 2018), since it has also been described to regulate protease activity of
104 *B. velezensis* DMB05 (Na *et al.*, 2023).

105 In this study, we isolated several novel *B. velezensis* strains from casing materials and
106 basidiomes that displayed antifungal activity to multiple mycoparasitic fungi. We characterise
107 these novel strains using phylogenetics and comparative genomics. We test three novel *B.*
108 *velezensis* strains for antimicrobial activity in crop via artificial inoculation on the casing
109 medium. In addition, both the survival rate of supplemented *B. velezensis*, and the equilibrium
110 of the endemic microbiota in this crop trial are assessed. Finally, we use LC-HRMS analysis
111 to identify and evaluate the secreted specialised metabolites of these *B. velezensis* strains that
112 correlate with their antifungal activity.

113 # Methods

114 ## Isolation of the cultivable bacterial microbiome

115 Cultivable bacteria were obtained from three casing materials used by the mushroom industry
116 in commercial crops (commercially available casing materials cquired from local providers:
117 black peat, based on peat moss (Euroveen B.V., BVB Substrates, Grubbenvorst, Limburg, The
118 Netherlands); blonde peat, based on Spaghnum peat moss (Valimex KF, Valimex SL, Valencia,
119 Spain); and a mixture of both casing materials (50 % each) (Euroveen B.V. and Valimex KF),
120 the physical and chemical characteristics of which have been previously reported (Carrasco *et*
121 *al.*, 2019). The methodology described by Aslani *et al.* (Aslani *et al.*, 2018) was implemented
122 to isolate bacteria from basidiomes of *Agaricus bisporus*.

123 ***Microbiome cultivation:*** i) for isolation of casing-colonising bacteria, 10 g of casing was
124 suspended in 100 mL of 0.1% sterile bacteriological peptone broth (Thermo Scientific
125 #LP0037B); ii) for isolation of basidiome-colonising bacteria, fresh and healthy closed
126 mushroom caps were externally disinfected by submerging them in 1% NaClO solution for 30
127 s and rinsing with sterile distilled water. 10 g of internal mushroom cap tissue was crushed and
128 homogenized with sterile pestle and mortar and suspended in 100 mL of 0.1% sterile
129 bacteriological peptone broth. Samples, either i) or ii) were added to Erlenmeyer flasks and
130 incubated in an orbital shaker-incubator (Ovan 1000001087, Badalona, Spain) at 120 rpm and
131 25 ºC for 10 min. The supernatant was transferred to a microtiter plate where successive 10-
132 fold dilutions (0.1% sterile bacteriological peptone broth) were dispensed. 100 µL of each
133 solution was transferred and homogeneously spread on growth media in 90 mm Petri dishes.
134 Media recipes employed in this work are described in Table S1.

135 ***Isolation and preservation of individual colonies:*** Exploring maximum diversity, one hundred
136 and forty-one individual colonies (Table S2) were re-isolated from plates based on colonial
137 morphology and transferred to plates containing LB Agar (LBA) medium. The re-isolated
138 colonies were incubated at 28 °C for 24-48 h. Single colonies were then added again to LB and
139 incubated in Erlenmeyer flasks between 25 and 28 °C in an orbital shaker at 150 rpm between
140 5 and 18 hours. The colony multiplication ratio was determined by spectrophotometer (Thermo
141 Fisher Scientific - Genesys 10-S) of the optical density in the culture broth at a wavelength of
142 600 nm (OD600). The fermentation was stopped when the absorbance at OD600 reached a
143 value of 1. The resulting cultures were re-suspended in 20% glycerol solution in sterile 2 mL
144 Eppendorf tubes. Finally, the tubes were stored at -80ºC (Panasonic MDF-U5386S-PE) until
145 further use.

146 Genomic extraction and sequencing

147 ***DNA extraction and Sanger sequencing of 16S rDNA:*** Single colonies were transferred to 10
148 mL LB at and incubated at 28 ºC on a platform shaker at 220 rpm for 24 h. The resulting
149 cultures were pelleted by centrifugation at 13,000 rpm for 1 min, and washed twice using
150 MilliQ water before aliquoting into 1.5 mL Eppendorf tubes. DNA was extracted from pellets
151 using the NucleoSpin Plant II, Mini kit for DNA from plants (MACHEREY-NAGEL GmbH
152 & Co. KG). The 27F and 1492R primers (Stackebrandt and Goodfellow, 1991) were used for
153 PCR amplification of 16S rDNA, which was performed using Phusion High-Fidelity PCR
154 Master Mix (Thermo Fisher, UK), with an initial denaturation of 98 °C for 30 s, followed by
155 30 cycles of 7 s at 98ºC, 30 s at 56 ºC, and 60 s at 72 ºC. A final extension of 7 min was used
156 before storage at 4 ºC. PCR products were prepared for sequencing by treatment with ExoSAP-
157 IT™ PCR Product Cleanup Reagent (Thermo Fisher, UK) and submitted to either Eurofins
158 (Luxembourg) or Source Bioscience (Nottingham, UK) for Sanger sequencing. Sequences

159 obtained using forward and reverse primers were aligned using MAFFT online
160 (https://mafft.cbrc.jp/alignment/server/). BLASTn searches were carried out using the NCBI
161 database (Camacho *et al.*, 2009).

162 ***Full genome sequencing and analysis:*** The full genomes of *Bacillus velezensis* CM5, CM19,
163 CM35, EM5 and EM39 were sequenced and annotated. Four 10 mL bacterial overnight cultures
164 (LB) were combined, washed twice in PBS and diluted to OD600 = 1, before aliquoting and
165 pelleting 10 mL and re-suspending in 0.5 mL of DNA shield (Zymo Research, Leyden, NL).
166 Genome sequencing of the three strains was carried out by Microbes NG, Birmingham, UK.
167 The downstream processing of sequence data was accomplished using several bioinformatics
168 tools: Reads were adapter trimmed using Trimmomatic 0.30 with a sliding window quality
169 cutoff of Q15 (Bolger *et al.*, 2014). De novo assembly was performed on samples using SPAdes
170 version 3.7 (Bankevich *et al.*, 2012), and contigs were annotated using Prokka 1.11 (Seemann,
171 2014). The Artemis genome browser was used for visualization and annotation (Rutherford *et*
172 *al.*, 2000). Assembly metrics were calculated by Quast (Gurevich *et al.*, 2013). A standard
173 analysis pipeline assigned reads to the closest available reference genome using Kraken (Wood
174 and Salzberg, 2014). The RAST annotation server and the SEED annotation environment were
175 used to annotate the prokaryotic genome (Aziz *et al.*, 2008; Aziz *et al.*, 2012). Further
176 comparative genomics of novel *B. velezensis* strains was carried out using the NCBI
177 Prokaryotic Genomes Automatic Annotation Pipeline (PGAAP) (Tatusova *et al.*, 2016).

178 The complete genome sequences of the *B. velezensis* strains reported in this paper have been
179 deposited in NCBI under the BioProject PRJNA1142391 with the genome accession numbers
180 CP168150 (CM19), CP168028 (CM5), CP168027 (CM35), CP168026 (EM5), CP168025
181 (EM39). To identify all genes containing single nucleotide polymorphisms (SNPs) in our novel
182 strains compared to the QST713 reference strain (Accession CP025079), we performed

183 comparative analyses using various computational tools and packages in R and Python. The
184 analysis workflow involved using BLASTn to detect differences in all genes present in the
185 QST713 reference genome. Genes with identified mismatches were then translated into their
186 corresponding amino acid sequences using the translate method from Biopython. These
187 translated sequences were subsequently compared using the BLASTp function to identify
188 amino acid substitutions. Coding sequences (CDS) with observed mismatches were further
189 analysed to ensure meaningful comparisons of functional protein-coding regions. BLAST Ring
190 Image Generator (BRIG) was employed for prokaryote genome comparisons (Alikhan *et al.*,
191 2011). The potential specialised metabolite profiles of the sequenced strains was evaluated by
192 antiSMASH (Blin *et al.*, 2021).

193 ***Phylogenetic analysis of* B. velezensis *strains:*** Phylogenetic analyses were performed using
194 five housekeeping genes: *gyrB*, *pgk*, *rpoB*, *rpoD,* and *tuf*. Genomes of comparative strains were
195 downloaded from NCBI and blasted against the annotated genes of the reference strain *B.*
196 *velezensis* FZB42. For our isolated strains of interest (CM5, CM19, CM35, CM18, CM20,
197 CM21), DNA extractions were carried out using the NucleoSpin Plant II, Mini kit for DNA
198 from plants (MACHEREY-NAGEL GmbH & Co. KG). Genes of interest were amplified by
199 PCR, carried out using Phusion® High-Fidelity DNA Polymerase master mix (NEB, Herts,
200 UK) and the primers listed in Table S4. PCR products were treated with ExoSAP as per the
201 manufacturer's instructions and submitted to Source Bioscience (UK) for Sanger sequencing.
202 Both FWD and RVS primers were used for sequencing reactions. Concatenated sequences were
203 used to build a phylogeny using Multiple Sequence Comparison by Log-Expectation
204 (MUSCLE) (Edgar, 2004). The phylogenetic tree was built using IQTREE (Nguyen *et al.*,
205 2015) using 1000 bootstrap replicates and set to automatically detect the optimal number of
206 threads. The resulting tree was visualised using iTOL (Letunic and Bork, 2021).

207 ## Transformation of *B. velezensis* CM19 with pHAPII gfp+

208 The plasmid pHAPII gfp+ (Cao et al., 2011) was extracted from a transformed strain of *B.*
209 *velezensis* QST713 (kindly provided by Romain Briandet, INRAE) using the NucleoSpin
210 Plasmid DNA extraction kit (Macherey-Nagel) using standard conditions. Subsequently, *B.*
211 *velezensis* CM19 cells were transformed using a room temperature electroporation protocol
212 (Morales-Ruiz *et al.*, 2019). In brief, competent cells were made by washing and suspending a
213 stationary phase culture of CM19 in phosphate buffered sucrose electroporation buffer (PEB:
214 272 mM sucrose, 1 mM $MgCl_2 \cdot 6H_2O$, 7 mM phosphate buffer, pH 7.4). Electroporation was
215 carried out in a 1 mm cuvette containing 400 ng plasmid and 90 µl of bacterial cells using a
216 single electric pulse at 620V, 200R and 25 µF. Cells were immediately resuspended in SOC
217 medium and incubated at 37 ºC without shaking for 4 h. After plating, a single transformed
218 colony was present after 24 h incubation at 28 ºC. Validation was carried out by plasmid
219 extraction (Macherey-Nagel™ NucleoSpin™ Plasmid) and submission for sequencing with
220 Plasmidsaurus (www.plasmidsaurus.com).

221 ## *In vitro* fungal inhibition assays

222 ***In vitro confrontation trials:*** Four fungal parasites were used for biocontrol assays:
223 *Trichoderma aggressivum* (TAV1), *Mycogone perniciosa* (M25) and *Cladobotryum*
224 *mycophilum* (CM13900) isolated from commercial mushroom crops in La Rioja (Spain); and
225 *Lecanicillium fungicola* (150/1), a UK isolate of medium virulence obtained from Warwick
226 HRI, UK (Banks *et al.*, 2019). All were stored as 25% glycerol stocks at -80 ºC. Before use,
227 fungi were plated onto PDA (potato dextrose agar) and grown for 3-7 days before scraping and
228 re-suspending in 30 mL MilliQ water in a 50 mL Falcon tube. Bacteria, also stored as 25%
229 glycerol stocks, were grown as overnight cultures in LB before use. For initial qualitative

230 biocontrol assessments, 10 µL of the fungal suspension was spotted on the centre of a PDA
231 plate. Four different 10 µL bacterial droplets from LB overnight cultures were spotted at a
232 distance of 20 mm from the fungal droplet. Plates were incubated in the dark at 25 ºC for 2 to
233 9 days depending on the parasite. Bacterial strains were scored as positively controlling fungal
234 parasites if a clear zone of clearing (halo) was observed around the bacterial colony. Each
235 bacterial strain was assessed at least twice. Since *B. velezensis* displayed biocontrol activity
236 against the four fungal parasites, further quantitative biocontrol plates were carried out using
237 just a single bacterial strain per plate. For this, 10 µL of the fungal cultures were co-inoculated
238 with bacterial droplets (at a distance of 30 mm) for between 1 and 6 days (depending on the
239 parasite). Plates were again incubated in the dark at 25 ºC for between 4 and 13 days.
240 Quantitative assessments were made by measuring zones of clearing. Each bacterial strain was
241 assessed in duplicate for at least two repeat experiments for each fungal parasite.

242 ***Spore germination assays*** Fully colonised PDA plates of the four fungal parasites were scraped
243 and resuspended in water through 8 layers of Miracloth. Using a haemocytometer, spore counts
244 were diluted to a concentration between $1 * 10^7$ and $1 * 10^8$ spores mL^{-1}. A 100 µL aliquot was
245 spread over a PDA plate and allowed to dry for 20 min. Subsequently, a 10 µL droplet of an
246 overnight, stationary culture of *B. velezensis* CM19 pHAPII gfp (in LB) was spotted onto the
247 centre of the PDA plate and allowed to dry. After 1-4 days of incubation at 28ºC, sections of
248 the agar plate around the bacterial droplet and halo of inhibition were cut and mounted on to a
249 microscope slide and covered with a cover slip. Fungal samples were stained for cell death
250 using a droplet of propidium iodide (PI, Thermo Fisher, R37108) at a final concentration of 1
251 µL mL^{-1} and assessed using a Leica TCS SP5 confocal microscope. Samples were scanned at
252 400 Hz (512 × 512 pixel images) using an argon laser with emission at 488 nm (intensity, 17%)
253 to excite GFP (detected at 510-530 nm) alongside a DPSS 561 nm laser (intensity, 35%) to

254 excite propidium iodide (detected at 625-645 nm). Unchallenged fungal parasites (without *B.*
255 *velezensis* confrontation) grown *in vitro* on PDA plates, stained for cell death as described were
256 assessed as control.

257 ***Effect of isolated bacteria on A. bisporus mycelium growth*:** *A. bisporus* was plated onto 2%
258 agar compost medium (70 g of powdered compost suspended in 1 L of water, autoclaved, then
259 filtered through Miracloth, and autoclaved again) and incubated in the dark for 7 days. 10 µL
260 droplets of bacteria from LB overnight cultures were spotted onto the plates at a distance of 3
261 cm from the original plating position of *A. bisporus.* Plates were divided into quadrants, and
262 four droplets were dispensed per plate (one per quadrant) with *A. bisporus* H15 inoculated in
263 the centre. After a further 7 days, photographs were taken and the radius of the distance between
264 the centre of the bacterial droplet and the edge of the fungal radial growth was measured.
265 Controls consisted of four droplets of LB broth free of bacteria per plate.

266 ***Toxicity of bacteria to A. bisporus sporocarp tissue:*** For assessment of sporocarp tissue
267 damage, 10 mm cubes of mushroom tissue were cut from mushroom caps. Bacteria from
268 overnight LB cultures were pipetted onto mushroom cubes at a rate of 100 µL per cube. Cubes
269 were photographed and assessed for browning using a 0-4 scale where: 0 was no effect; 1 light
270 tissue scarring; 2 light browning; 3 heavy browning; and 4 being either black or dark brown
271 with obvious seepage. Control treatments consisted of mushroom cubes treated with sterile LB
272 broth at a rate of 100 µL per cube.

273 Biocontrol activity of *B. velezensis* in a crop trial infected with *L. fungicola*

274 ***Bacterial inoculum preparation*:** Bacteria were grown overnight in LB broth. Cultures with
275 OD600 > 0.7 were used to inoculate a bioreactor to produce bacterial batches through liquid
276 fermentation. A 5L Biostat A fermenter (Sartorius, Germany) was then used to culture large

277 bacterial batches (T = 28 ºC, pH = 7, critical oxygen concentration = 10-50% of air saturation,
278 time: 7-8 h to an OD600 = 1). The resulting broth was centrifuged at 4500 rpm for 10 min at
279 10ºC (Sorvall Legend XTR Centrifuge, Thermo Scientific, Waltham, MA, USA). The
280 supernatant was removed and the pellet washed twice with PBS (phosphate buffer, pH = 7.4)
281 before resuspension in 100 mL of 10% skim milk and 10% saccharose solution as a
282 cryoprotector. The frozen solution was freeze-dried and pulverized into ready to use water
283 soluble powder. The viable concentrations were confirmed by plating serial dilutions in sterile
284 water onto LB.

285 ***Crop Trial:*** The crop trial was conducted in an experimental growth chamber equipped with
286 climate control (Mod. IGCS 1500 HR LED, Ibercex, Spain) according to standard practices
287 used in mushroom farms. The trial was performed with a randomized block design using 32
288 blocks (0.04 m^2 crop surface) of 1250 g phase III compost (Sylvan H15 - supplemented with
289 Mylo Pro and Champfood) and 750 g of black casing (CNC, Valimex or Euroveen) at
290 maximum water holding capacity. The six treatment groups are shown in Table **1** (1: Control
291 (water) + *L. fungicola* (Lf); 2: Control (water) – Lf; 3: CM5 + Lf; 4: CM19 + Lf; 5: CM35 +
292 Lf;6: Prochloraz-Mn (PCL) + Lf). Treatment with prochloraz-Mn (PCL), as a fungicide
293 control, was carried out on day 4 after casing (d4), inoculation of bacteria was carried out on
294 d5, infection with Lf strain 150/1 (Banks *et al.*, 2019) was carried out on d10. *L. fungicola*
295 inoculum was prepared as described by Gea et al. (Gea *et al.*, 2014) on the day of inoculation
296 and applied by spraying the top of the casing layer at a dose of 10^6 conidia m^{-2} using a
297 suspension of 20 mL of 2×10^6 conidia L^{-1}. Bacterial suspensions were applied on top of the
298 casing layer using 20 mL of a 2×10^9 cfu L^{-1} suspension in tap water for a final rate of 10^9 cfu
299 m^{-2}.

300 For analysis of disease and biological efficiency, healthy and diseased mushrooms and bubbles
301 were scored at the end of the first and second crop flushes. For PLFA analysis in the casing
302 materials, four timepoints were assessed: d0 (Beginning of trial), day 10 (Fully colonized
303 casing), d21 (Fructification of first flush), and d29 (End of first flush). 1: Raw casing material
304 (beginning of the trial, casing free of host), 2: Casing fully colonised by *Agaricus* mycelium
305 (end of spawn running, day 10), 3: Casing during mushroom fructification (fructification of 1st
306 flush, day 21); 4: Casing sample taken by the end of 1st flush (end of the harvest, day 29).

307 **Analysis of PLFAs:** Casing microbial biomass and structure were determined using
308 phospholipid fatty acid (PLFA) analysis (Frostegård *et al.*, 1993) and fatty acid methyl esters
309 (FAMEs) were analysed by gas chromatography. The total microbial biomass was estimated
310 by the total sum of PLFAs and expressed as nmol g^{-1}. Specific PLFAs were used as biomarkers
311 to quantify the relative abundance of Gram-negative bacteria (monounsaturated fatty acids and
312 cyclopropyl 17:0), Gram-positive bacteria (iso and anteiso saturated branched chain fatty
313 acids), Actinobacteria (10-methyl fatty acids) and fungi (18:2 ω6 cis and 16:1w5) (Zelles,
314 1999). ***Statistical Analysis:*** Total biomass of bacteria and fungi determined by PLFAs was
315 submitted for the analysis of variance (ANOVA) by previous Levene variance homogeneity
316 tests to determine significant differences between samples. Means were compared by either
317 Tukey or Games-Howell post hoc test based on whether variance of homogeneity was met,
318 respectively ($p < 0.05$). ANOVA and post hoc tests were performed by IBM SPSS Statistics
319 v24 software package (SPSS Inc. Chicago, USA). Principal component analysis (PCA) was
320 performed with PAST v3.15 software (Hammer *et al.*, 2011).

321 ## TaqMan assays for *B. velezensis* strains (CM19, CM5 and CM35)

322 **DNA extraction:** Bacteria were collected with a loop from the agar surface of 90 mm diameter
323 tryptic soy agar (TSA) plates into a 2 mL tube and used for DNA extraction. The Wizard
324 Genomic DNA purification kit (Promega) was used for DNA extraction. DNA yield was
325 determined by using the Qubit ds DNA HS assay kit with the Qubit Fluorometer (Life
326 Technologies).

327 **TaqMan design:** To design a TaqMan assay that specifically detects the *B. velezensis* target
328 strains, we made use of the whole chromosomal genome sequence. Potential target sites were
329 identified using CLC genomic workbench (Qiagen, Aarhus, DK). The genome sequences of
330 the target were dissected in 500 bp-long sequences. These sequences were mapped to
331 sequences of *B. velezensis* QST713 (CFSAN0334339), a non-target strain isolated from
332 agricultural soil (Pandin *et al.*, 2018) (CLC mapping settings: length fraction: 0.85, similarity
333 fraction: 0.85, global alignment: no), thus removing sequences that mapped to any of the non-
334 target strains. To assist the final selection and design step, these (unmapped) sequences were
335 added as a track list to the target strain genome.

336 Before proceeding to the design step, the candidate regions were checked for sequence
337 similarity with non-target organisms using BLASTn (NCBI) (Camacho *et al.*, 2009). At least
338 six sets of primer/probe combinations were designed per target on 500 bp target-specific
339 fragments using primer quest tool of Integrated DNA Technologies (IDT, Leuven, Belgium)
340 with default settings. Two sets of primer/probe combinations were selected for the design of
341 the final triplex TaqMan assay, targeting different genes, based on the kinetics.

342 **Specificity of the TaqMan assays:** The specificity of the assays was tested using genomic
343 DNA of 27 strains (Table S6). For most strains 0.5 ng of purified DNA was used, but for some

344 strains a suspension of 10^9- 10^{10} cells/mL was boiled for 10 min in 150 µL MilliQ water (MQ)
345 prior to testing. For each TaqMan assay 2 µL of DNA or the boiled suspensions was mixed
346 with 2 µL reaction mix containing PerfeCTa multiplex qPCR ToughMix 5x (Quantabio,
347 Beverly, USA), 100 nM probe and 300 nM of each forward and reverse primer. The reactions
348 were performed in a 12K Flex QuantStudio or a QuantStudio 5 Real-Time PCR system
349 (Applied biosystems) using the following conditions: 95 °C for 2 min; 40 cycles of 95 °C for
350 15 s followed by 60 °C for 60 s. Analysis of the data was done by automatic threshold
351 calculation within the Applied Biosystems software. A Ct value ≤ 35 was considered positive.

352 The specificity and usability were further tested using constituents of casing soils or casing
353 soils of various compositions. DNA was extracted from 10 g of material using the DNeasy
354 PowerMax Soil kit (Qiagen, Germany) according to the manufacturer's protocol. TaqMan
355 assays were performed as described above with 2 µL DNA.

356 **Triplex TaqMan design:** The two simplex assays for the target bacteria were combined with
357 an assay that quantifies *Xanthomonas campestris* pv. *campestris* (Xcc) into a triplex TaqMan
358 (Table S7) (Köhl *et al.*, 2011; Taparia et al., 2020). For each group of biostimulants, a triplex
359 TaqMan assay was designed with two target-specific assays, each with its own dye (Cy5 or
360 FAM) and an amplification and extraction control (*X. campestris*), labelled with HEX. The
361 triplex TaqMan was performed using the same PCR conditions and materials as the simplex
362 tests, with 100 nM probe and 300 nM of each primer in a total volume of 25 µL.

363 **Limit of detection of the assays:** The limit of detection for the triplex assays designed for *B.*
364 *velezensis* strains CM19, CM5 and CM35 (Table S12-S15) was determined in two casing soils,
365 i.e. in peat and steamed spent casing soil. 100 µL of a ten-fold serial dilution of 3-days old
366 cultures of the strains in Ringers in a PowerBead Pro tube was mixed with 250 mg of the

367 casings ($4 \times 10^7 – 4 \times 10^1$ cells g^{-1} of casing soil). Casing soils with 100 µL Ringers without
368 supplemented bacteria served as a control. A volume of 100 µL of a suspension of *X.*
369 *campestris* (Xcc) of 10^6 cell mL^{-1} was added to each sample as extraction and amplification
370 control. The soils were subsequently freeze dried overnight and shaken for 2 times 90 seconds
371 in a paint shaker. DNA was extracted using a DNeasy Power Soil Pro Kit according to the
372 manufacturer's instructions. The triplex TaqMan assay was executed as described above with
373 0.75 µL of each primer (10 µM) and 0.75 µL of each probe (10 µM), labelled with FAM, Cy5
374 (for target specific probes) or HEX (for Xcc).

375 Surfactant activity and lipopeptide production

376 ***Surfactant production:*** *B. velezensis* strains were cultured overnight in Optimised Medium
377 (OM, Table S1) and standardised to OD600 = 1. Droplets (10 µL) were pipetted onto the lid of
378 a Greiner CELLSTAR® 96 well plate, allowed to sit for 2 min, and measured using an eye
379 piece graticule on a ZEISS dissecting microscope. The mean droplet diameters of three
380 independent experiments, each containing 2 droplets, were assessed for differences to an OM
381 only control using Students' T-Test.

382 ***Lipopeptide fraction collection:*** Lipopeptides were extracted from 600 mL liquid cultures of
383 CM19, which were incubated at 30 ºC for 24 h in Optimized Medium (Table S1). Samples
384 were centrifuged at 10,000 g for 10 min to remove the cell pellet. The resulting solution was
385 acidified by addition of concentrated HCl to pH 2.0 and precipitated overnight at 4 °C. The
386 solution was again centrifuged at 10,000 g for 15 min at 4 °C. The pellet was resuspended in
387 10 mL methanol while shaking for 2 h continuously. The resulting solution was filtered through
388 a 0.4 µm filter and concentrated by evaporation to a final volume of 1 mL methanol. The

389 methanol suspension was then used for the confrontation assays by saturating the discs by
390 briefly incubating them in the solution.

391 ***Extraction of agar plates for targeted metabolic profiling:*** The *B. velezensis* strains CM5,
392 CM19 and CM35 were cultivated on LB agar plates for 5 days at 28 ºC. For each strain, five
393 agar plates were extracted and pooled. Firstly, bacterial agar plates and negative control plates
394 (unseeded LB agar plates) were crushed and suspended in 20 mL HPLC-grade MeOH (J. T.
395 Baker, Deventer, The Netherlands). The mixture was transferred to a beaker, 30 mL of fresh
396 MeOH was added (total volume 50 mL) and further processed in an ultrasonic bath (Sonorex
397 Longlife, Bandelin, Berlin, Germany). After 10 minutes, the mixture was filtered and the wash
398 repeated. The filtrate was concentrated to dryness under reduced pressure at 35 °C in a rotary
399 evaporator (Laborota 4001 Efficient, Heidolph, Schwabach, Germany) operating at 100 rpm.
400 The residue obtained was dissolved in 1 mL HPLC-grade MeOH, centrifuged at 8000 rpm for
401 5 min, and measured by HPLC-HRMS.

402 ***High-performance liquid chromatography-high resolution mass spectrometry (HPLC-***
403 ***HRMS):*** The extracts were analysed on a LTQ Orbitrap XL mass spectrometer (Thermo
404 Scientific, USA) equipped with a HESI-II source coupled to Agilent (Santa Clara, USA) 1200
405 HPLC system including pump, PDA detector, column oven and autosampler. A Luna C_{18} (2)
406 column (50 × 3 mm, 3 µm particle size) from Phenomenex (Torrance, USA) was used for the
407 HPLC-HRMS and an Aeris PEPTIDE XB-C_{18} (150 × 2.1 mm, 3.6 µm particle size) for $HRMS^n$
408 measurements with a H_2O (+0.1% FA) (A) and CH_3OH (+0.1% FA) (B) gradient (flow rate
409 350 µL min^{-1}). The gradient program was optimized and set as follows: 5% B isocratic for 2
410 min, linear gradient from 5% to 100% B over 24 min, 100% B isocratic for 6 min, the system
411 returned within 0.5 min to initial conditions of 95% A and was equilibrated for 3 min. For
412 selected target fengycins and their $HRMS^n$ measurements, the gradient was slightly modified:

413 5% B isocratic for 2 min, linear gradient from 5% to 90% B over 8 min and then over 20 min
414 up to 100%, the system returned within 0.5 min to initial conditions of 95% A and was
415 equilibrated for 3 min. The mass spectrometer was operated in positive mode with a nominal
416 mass resolving power of 60000 at *m/z* 400 with a scan rate of 1 Hz, and *N*-butyl
417 benzenesulfonamide was used as lock mass ($[M + H]^+$; *m/z* 214.08963 for full scans and a
418 mass range from *m/z* 160-1600. Helium served as collision gas and N_2 was used as sheath and
419 auxiliary gas. The $HRMS^n$ measurements were performed with collision-induced dissociation
420 of 42 eV. An authentic reference standard of fengycin (≥ 90%) was procured from Sigma-
421 Aldrich (Steinheim, Germany). The analyses were performed using Xcalibur software v. 2.2
422 SP1.48. (Thermo Scientific, Bremen, Germany). The acquired masses were sorted by intensity
423 (I > 1.00E3). A maximum mass tolerance of 2 ppm was accepted. Background subtraction was
424 performed as required using Xcalibur software v. 2.2 SP1.48. (Thermo Scientific, Bremen,
425 Germany).

426 **Results**

427 ***Bacillus velezensis* strains isolated from mushroom casing microbiome display**
428 **antimicrobial activity towards mushroom mycoparasites.**

429 One hundred and forty-one strains belonging to the cultivable bacterial microbiome from the
430 peat casing layer and basidiomes of *Agaricus bisporus* were isolated and classified using
431 BLASTn (blast.ncbi.nlm.nih.gov) based on their 16S rDNA sequences (Table S2). A wide
432 range of bacterial species were isolated of which *Bacillus* spp. and *Pseudomonas* spp. were
433 most highly represented (Figure **1**A). Initial antifungal confrontation assays (Table S3)
434 indicated that strains belonging to the species *B. velezensis* showed a particularly high degree
435 of antagonism towards four major fungal parasites of *A. bisporus*: *Trichoderma aggressivum,*

436 *Mycogone perniciosa, Lecanicillium fungicola*, and *Cladobotryum mycophilum* - these strains
437 were selected for further phenotypic analysis (Figure 1B and Table **2**).

438 Nine strains of *B. velezensis,* and a control strain CM26 (BLASTn 98.47% *Bacillus*
439 *oceanisediminis*) which failed to show antagonistic activity in initial assays, were tested for
440 antifungal activity against four fungal parasites of the cultivated button mushroom *Agaricus*
441 *bisporus* in confrontation assays: *L. fungicola* (150/1); *T. aggressivum* (TAV1); *M. perniciosa*
442 (M25); and *C. mycophilum* (CM13900). All of the *B. velezensis* strains tested produced
443 statistically significant levels of inhibition with only CM26 showing significantly different
444 inhibition (Figure 2A, 4B; ONE WAY ANOVA, *C. mycophilum* $p < 0.001$, *L. fungicola* $p <$
445 0.001, *M. perniciosa* $p = 0.139$, *T. aggressivum* $p < 0.001$. Letters are results of post-hoc
446 TUKEY test showing significant differences $p < 0.05$).

447 *B. velezensis* CM19 was selected as a representative strain and transformed with the plasmid
448 pHAPII gfp. Transformed bacteria were confirmed to express GFP and used to examine the
449 effect of CM19 on conidial and hyphal viability and morphology *in vitro* (Pandin *et al.*, 2017).
450 Live dead staining with propidium iodide (PI) was used to study the effect of CM19 on spore
451 survival and germination (Figure 2C, D, E). Spores were classified as dead if either fully stained
452 with PI or observed to be hollow/lysed cells. In many cases spores were deemed to have
453 germinated but resulting hyphae were also found to be stained or lysed.

454 For a strain to be an effective biocontrol agent against mycoparasitic fungi it is important that
455 strains are not only antagonistic to mycoparasites, but also show low toxicity to hyphae and
456 sporocarps of *A. bisporus.* Strains were tested for antagonism to *A. bisporus* in both
457 confrontation assays and in mushroom cube assays, where cubes of sporocarp tissue were
458 exposed to dense suspensions of bacteria, a standard assay for mushroom pathogenic bacteria

459 such as *Pseudomonas tolaasii,* which was used as a positive control (Godfrey *et al.*, 2001). The
460 majority of the selected strains exhibited limited antagonism to *A. bisporus* and did not cause
461 significant browning and collapse of sporocarp tissue, making them promising candidates as
462 biocontrol agents (Figure 2F and Figure S1).

463 **Mushroom casing isolates of *Bacillus velezensis* are closely related to the commercial**
464 **biocontrol strain *B. velezensis* QST713**

465 Further phylogenetic analysis was carried out for five *B. velezensis* strains isolated from casing
466 alongside the commercially used 'Serenade' *B. velezensis* strain QST713 using primers for the
467 housekeeping genes *rpoB*, *tuf, rpoD*, *pgk* and *gyrB* (Table S4). The nucleotide sequences
468 obtained were used to build a phylogenetic tree of the isolated *B. velezensis* strains alongside
469 other *Bacillus* spp. for which sequence data is available in the NCBI database. The results
470 showed a clear delineation into three clades: *B. amyloliquefaciens*, *B. velezensis* and *B. subtilis*
471 Figure 1B, which is consistent with previous reports (Fan *et al.*, 2017; Pandin *et al.*, 2018).
472 Four of the strains (CM5, CM19, CM35 and EM5), were found to be within the *B. velezensis*
473 clade and to be very closely related to each other and to the commercial biocontrol agent
474 QST713.

475 Five *B. velezensis* casing isolates (CM5, CM19, CM35, EM5 and EM39) were selected for
476 genome sequencing, which confirmed that these four strains had very high levels of homology
477 compared to QST713, returning a percentage identity of 99.99% when analysed using NCBI
478 PGAAP (Table **2**). A full breakdown of all genes containing SNPs compared to QST713 and
479 how these affect the relevant amino acid sequences can be found in Table S5.

480 **Fengycins are the most abundant anti-microbial lipopeptides produced by**
481 **casing isolates of *Bacillus velezensis in vitro.***

482 We used the prediction software antiSMASH to identify potential gene clusters involved in
483 specialised metabolite biosynthesis that could be involved in the antagonistic behaviour
484 displayed by the casing isolates of *B. velezensis* (Figure 2). This analysis identified multiple
485 gene clusters (Table 3) with homology to clusters previously shown to encode the enzymatic
486 machinery for synthesis of the nonribosomal peptides surfactin, fengycin, bacillibactin, and
487 bacilysin and the antimicrobial polyketides bacillaene, difficidin, and macrolactin. Surfactin
488 and fengycin are lipopeptides known to have both antimicrobial and surfactant activity (Sur *et*
489 *al.*, 2018; Gilliard *et al.*, 2024) while bacillibactin is an iron-chelating siderophore (Qin *et al.*,
490 2019).

491 Surfactant production by the selected *B. velezensis* strains was evaluated using a droplet
492 diameter assay (Akpa *et al.*, 2001). All *B. velezensis* strains had significantly different droplet
493 diameters compared to the LB-only control (A), confirming that these strains produce factors
494 both with antimicrobial and surfactant activity.

495 The identity of the specialised metabolites produced by CM5, CM19 and CM35 was further
496 investigated using bioinformatics- and literature-guided targeted metabolic profiling by high-
497 performance liquid chromatography-high-resolution mass spectrometry (HPLC-HRMS).

498 Targeted metabolic profiling revealed production of fengycin (1xCO,1xOH,Ala:R1=13C)
499 (Figure 4) by all three bacterial strains under the cultivation conditions tested. Fengycins A and
500 B differ in the amino acid alanine (A) or valine (B) at the sixth position. Identification of the
501 fengycin was achieved by comparison with an authentic reference standard and referencing the
502 mass spectral fragmentation pathway with literature (Wang *et al.*, 2004; Ma *et al.*, 2016). Other

503 target compounds from antiSMASH prediction (see Table S9), including macrolactins, were
504 not produced under the tested conditions (i.e., < limit of detection (LOD)).

505 The application of *Bacillus velezensis* strains to mushroom crops was 506 ineffective in limiting disease caused by the dry bubble parasite 507 *Lecanicillium fungicola.*

508 Three *B. velezensis* strain (CM5, CM19, CM35) were taken forward for crop trials. Application
509 doses were selected based on preliminary results observed using a small growth chamber and
510 the application dose approved for the commercial product Serenade ASO® (*Bacillus velezensis*
511 QST 713) in Spain: 5.4 x 10^8 cfu/100 kg compost against *Trichoderma aggressivum* (MAPA,
512 2025). The crop trials were designed to assess (i) effects of the treatment on the biological
513 efficiency of the crop, and (ii) biocontrol effects against the fungal parasite *L. fungicola*.

514 Disease was successfully established following inoculation with LF and statistically significant
515 differences between control groups (+LF and –LF) were detected (Figure 5A), confirming that
516 artificial inoculation with LF affected yield. The control inoculated with LF (Figure 5A) was
517 the least productive in terms of biological efficiency, and treatment with a single dose of CM19
518 was the most productive. However, differences between control and *B. velezensis* treatments
519 were not found to be significant ($p > 0.05$) in the first flush, second flush or total cropping cycle
520 (Figure 5A). As expected, the use of prochloraz-Mn (PCL) was found to significantly reduce
521 disease in both the first and second flush.

522 Phospholipid fatty acid analysis (PLFA)

523 To further examine whether supplementation with *B. velezensis* affected the mushroom casing
524 microbiota, phospholipid fatty acid (PLFA) analysis was carried out to evaluate the relationship

525 between microbial biomass and community structure in the commercial casing substrate during
526 the crop trial at different stages of mushroom cropping. PLFA quantifies total microbial
527 biomass and specific microbial groups (gram-positive bacteria, gram-negative bacteria,
528 Actinomycetes, and total fungi) to provide a general overview of microbial structure and
529 dynamics (52) (Table S8).

530 The total microbial biomass in the casing soil increased significantly over time at the different
531 stages of the crop. Specifically, microbial PLFAs in the casing soil were 3.4, 5.8 and 9.5 times
532 higher in the control treatment at the stages of mycelia penetration in the casing layer (initial
533 cropping stage), first flush primordia formation (start of fructification), and first flush
534 mushroom growth (end of harvest), respectively, compared to the casing soil (raw material)
535 (Figure 6A).

536 The proportion of PFLAs associated with bacterial populations in the casing soil decreased
537 over time while the proportion of fungal PLFAs increased. Fungal PLFAs were relatively more
538 abundant than bacterial PLFAs by the end of the first flush (day 29). Gram-negative and gram-
539 positive bacterial fatty acids were higher during the initial cropping stage compared to the other
540 stages (Figure 6B,C). However, the relative abundance of gram-negative bacterial PLFAs was
541 higher than gram-positive ones across all cropping stages. Actinomycete populations were
542 significantly lower compared to the other bacterial groups (gram-negative and gram-positive
543 bacteria) during all stages of mushroom growth (Figure 6D).

544 The casing soils treated with *B. velezensis* strains showed significant differences in microbial
545 biomass and composition within the four microbial groups analysed and across the different
546 cropping stages (Figure 6E). The highest relative abundance of bacterial PLFAs at the flushing

547 stage was observed in the control treatment supplemented with *L. fungicola* (+), while the
548 highest relative abundance of fungal PLFAs was observed in treatment 5 (strain CM35).

549 TaqMan assays for *B. velezensis* indicate low persistence of biostimulants 550 following supplementation to mushroom crops

551 To investigate whether the lack of a positive biocontrol effect for *B. velezensis* in crop could
552 be linked to low persistence of the biostimulants in mushroom casing we developed a specific
553 TaqMan assay to track the population density of *B. velezensis* when supplemented to casing
554 soil. The whole genome sequence of *B. velezensis* strains CM19, CM5 and CM35 are almost
555 identical and only showed a limited number of SNPs (Table S5). It was technically impossible
556 to differentiate the strains in a TaqMan assay based on a single SNP, and thus we decided to
557 design an assay for a subgroup of this species that includes the strains CM5, CM19 and CM35,
558 together with other closely related *B. velezensis* strains. Two *B. velezensis* subgroup-specific
559 assays, targeting different genes, were combined into a triplex assay with a specific assay for
560 *Xanthomonas campestris* pv. *campestris*, which was used as extraction and amplification
561 control (Table S7).

562 The two *B. velezensis* subgroup-specific assays in the triplex assay gave a positive result with
563 the three target strains and with CM18, CM20, CM21 and EM5, which all clustered in the same
564 subgroup (Figure S2B; Table S14), but not with other *B. velezensis* strains outside this
565 subgroup, such as *B. velezensis* EM39.

566 Despite showing high specificity, the assay showed low sensitivity, giving a positive result
567 only for cells present at 10^4 cfu/g of casing soil when used to detect cells present in exponential
568 cultures, and 10^7 cfu/g of soil for samples from stationary cultures (Figure 7C), potentially
569 indicating low efficiency of DNA extraction from spores. When used to detect *B. velezensis* in

570 casing samples, the bacteria could only be detected on the day of application (days 1 and 18
571 after casing; Figure 7A, B), suggesting low persistence and/or conversion to spores following
572 supplementation.

573 **Discussion**

574 The horticultural activity of button mushroom cultivation includes different agronomic
575 operations: a) production of a selective substrate through a process of composting; b)
576 inoculation with the selected *A. bisporus* strain; c) casing of colonised substrate, commonly
577 with non-sterile, peat-based material; d) fruiting and harvest (Carrasco *et al.*, 2021). The casing
578 layer is a microbe-rich environment where mushroom fructification occurs, driven by the action
579 of beneficial bacteria (Braat *et al.*, 2022), and is also considered to be the main infection site
580 for mycoparasites, the most damaging biotic disorders of mushroom crops (Carrasco *et al.*,
581 2021; Gea et al., 2021). The microbiota present in casing soil therefore plays a key role in both
582 promotion of mushroom fructification and disease development or disease suppression. The
583 aim of this work was to isolate and characterize bacteria that are naturally resident in casing
584 soil or live in association with mushroom basidiomes, to show antifungal activity of these
585 bacteria towards economically important mycoparasites; to investigate the mechanistic basis
586 of this antifungal activity, and to investigate the potential of these bacteria as biocontrol agents
587 in crop.

588 Several strains of *B. velezensis*, including CM5, CM19 and CM35 (included in a published
589 patent (Carrasco and Preston, 2023)), isolated from commercial casing material, and *B.*
590 *velezensis* EM5 and EM39, isolated from mushroom basidiomes, have been identified and
591 demonstrated to possess antifungal activity towards four of the most damaging mycoparasites
592 (*C. mycophilum, L. fungicola, M. perniciosa* and *T. aggressivum*). The antifungal activity

593 observed in our strains is consistent with the potential biocontrol activity reported in other
594 strains, including *B. velezensis* Kos isolated from mushroom casing environment at Teagasc,
595 Ireland (Kosanović *et al.*, 2021; Clarke *et al.*, 2022a, 2022b) and the commercial biocontrol
596 agent *B. velezensis* QST713, isolated from soil in a peach tree orchard in Fresno County,
597 California (USA) (Anastassiadou *et al.*, 2021).

598 Importantly, *B. velezensis* CM5, CM19 and CM35 showed limited toxicity to *A. bisporus in*
599 *vitro* and did not show a deleterious effect on the mushroom mycelium at the dose applied in
600 crop (10^9 cfu m^{-2}). However, compared to an established chemical treatment (PCL), none of
601 the three strains provided effective control of the dry bubble parasite *L. fungicola* in a crop trial
602 (Figure **5**B). According to previous published results, the commercial formulations of *B.*
603 *velezensis* strain QST 713 (Serenade®, Bayer Crop Science, Valencia, Spain) and *Bacillus*
604 *amyloliquefaciens* subsp. *plantarum* strain D747 (Amylo-X®, Certis Europe, Alicante, Spain)
605 also offered poor control of wet bubble disease in crop trials, with their effectiveness further
606 reduced under high pressure of parasite inoculum (Navarro *et al.*, 2023). Similarly, *B.*
607 *velezensis* QST 713 did not control cobweb disease in a crop trial artificially infected by *C.*
608 *mycophilum* isolate 1546 while *B. velezensis* Kos 96h culture filtrate reached 30–40% efficacy
609 (Clarke *et al.*, 2024). This indicates that parasite identity, inoculum density and disease pressure
610 may all affect the outcome of control treatments, and that beneficial effects may largely due to
611 antimicrobial compounds present in the culture (or culture filtrate) at the time of application.
612 Our trial used a high inoculum density of *L. fungicola* compared to the natural parasite pressure
613 in commercial facilities. It is possible that at a lower inoculum density, a higher dose of *B.*
614 *velezensis* applied to the crop, or by optimising culture conditions and inoculum design to
615 increase production of antimicrobial compounds, both prior to and upon application to the crop,
616 a better disease control will be achieved. However, in pilot assays, at the highest doses used (>

617 10^{10} cfu/m^2), *B. velezensis* was observed to have a potential deleterious effect on *A. bisporus*
618 colonisation of casing soil (our unpublished results), and therefore it is likely be necessary to
619 further optimise the dose and formulation of *B. velezensis* applied to the crop to achieve optimal
620 results.

621 Selective TaqMan assays were developed to study the population dynamics of *B. velezensis* in
622 crop. The availability of two TaqMan assays per target organism in combination with an assay
623 for extraction and amplification allows specific and reliable detection of the targets in multiplex
624 set-up. However, the LOD was $\leq 4 \times 10^5$ cells per mL in casing soils, which only allows studies
625 of the population dynamics in situations in which relatively high densities of the *B. velezensis*
626 are supplemented to or persist in the casings. Additionally, we observed low efficiency
627 detection of bacteria that had entered stationary phase, potentially linked to challenges with
628 efficient extraction of DNA from spores.

629 When the TaqMan assays were applied to crop trial samples, we found that the target strains
630 could only be reliably detected on the day of application. This suggests that their population
631 declines rapidly following inoculation, or that the bacteria have entered stationary phase and
632 formed spores, in which case the TaqMan assay may significantly under-report their abundance
633 in casing samples. Since *B. velezensis* must adapt to a complex environment, optimizing the
634 formulation or antimicrobial activity of *B. velezensis* based products is key to improve stability,
635 shelf-life and deliver biocontrol activity (Kenfaoui *et al.*, 2024)..

636 As previously reported (Carrasco *et al.*, 2019, 2020), we observed that microbiome structure
637 changes along the process of mushroom cultivation. PLFA analyses confirmed that the
638 cultivation stage of *A. bisporus* correlated with significant changes in the composition of the
639 microbial communities in the casing, where the bacterial population, particularly gram-

640 negative bacteria, have been reported to play a fundamental role during the early development
641 of the mushroom primordia. The highest microbial biomass was found in the casing soil at the
642 end of fructification, indicating changes in microbial structure associated with mushroom
643 mycelium growth. The increase in the microbial population, with respect to both bacterial and
644 fungal biomass, correlated with the mycelial growth of *A. bisporus*, in accordance with
645 previous results (Chen *et al.*, 2009; Carrasco *et al*., 2020). The increase in the bacterial
646 population may be attributable to metabolites released during the development of fruiting
647 bodies, which alter nutrient composition and influence the diversity of microbial communities
648 in mushroom casing (Zhao *et al*., 2022).

649 Interestingly, application of *B. velezensis* strains in crop had a positive effect on both the gram-
650 negative and gram-positive communities suggesting that in addition to directly inhibiting
651 mycoparasitic fungi, it could have a synergistic effect on mushroom growth by promoting the
652 proliferation of disease-suppressing or fructification-promoting bacteria, perhaps through an
653 anti-competitor effect or by releasing nutrients through lysis of susceptible organisms. The
654 higher amount of gram negative compared to gram positive bacteria in all cropping stages is
655 consistent with the hypothesis that gram negative bacteria play a key role in stimulating the
656 initiation of mushroom sporophores (Chen *et al.*, 2009). Gram-negative bacteria, particularly
657 members of the Pseudomonadales such as *Pseudomonas putida* have been identified as major
658 microbial stimulants for sporophore formation in the casing layer, potentially by metabolizing
659 volatile compounds in the casing soil that would otherwise inhibit sporophore initiation,
660 thereby creating conditions conducive to sporophore formation (Rainey, 1989; Noble *et al.*,
661 2003).

662 Actinomycetes are sensitive to environmental changes, such as shifts in temperature, pH, and
663 moisture levels, which occur during mushroom cultivation (Lacey, 1997; Akond *et al.*, 2016).

664 These fluctuations could adversely affect their survival and proliferation, leading to lower
665 populations compared to more resilient bacterial groups. Besides, the casing layer is rich in
666 microbial diversity, leading to competition for nutrients and space. Actinomycetes may be
667 outcompeted by faster-growing bacteria, such as *Pseudomonas* spp., resulting in their reduced
668 presence during mushroom growth stages (Rainey, 1989; Noble *et al.*, 2003).

669 *B. velezensis* CM5, CM19, CM35, EM5 and EM39 all showed antimicrobial activity against
670 mycoparasites causing cobweb (*C. mycophilum*), dry bubble (*L. fungicola*), wet bubble (*M.*
671 *perniciosa*) and green mould disease (*T. aggressivum*) *in vitro*. Similarly, Clarke et al. (Clarke
672 *et al.*, 2022a, 2022b) have reported that *B. velezensis* Kos has antimicrobial activity against *C.*
673 *mycophilum* and *L. fungicola*. Genome sequencing identified several gene clusters in these
674 strains that could direct the production of a range of non-ribosomal peptide and polyketide
675 antifungal compounds. However, analyses of the specialised metabolites produced *in vitro*
676 identified lipopeptides known as fengycins as the major non-ribosomal peptides produced by
677 these strains in pure culture under the conditions tested. It therefore seems likely that fengycins
678 are the primary factors responsible for both the anti-fungal activity and the surfactant activity
679 observed for these bacteria *in vitro.* However, we cannot exclude the possibility that some of
680 the anti-fungal compounds produced by these bacteria are only produced in the presence of
681 other microorganisms, or that these bacteria express a different arsenal of anti-microbial factors
682 during colonisation of mushroom casing or sporocarps. Previous studies have shown that many
683 gene clusters encoding anti-microbial factors remain silent in standard culture conditions.
684 These cryptic biosynthetic genes may only be induced during co-culture or specific
685 environmental conditions (Ochi , 2017).

686 The chemical structure of the fengycin analogues produced has been determined for CM5,
687 CM19 and CM35 when cultured *in vitro*. Interestingly, despite the high degree of similarity

688 between these strains at a genomic level CM19 showed higher production of the fengycin
689 analogue *in vitro*, suggesting that epigenetic differences or one or more of the SNPs detected
690 (Table S16) could be responsible for this differential production.

691 Fengycin is known to exert its anti-fungal activity by assembling into pore-forming complexes
692 that target fungal cell membranes (Zakharova *et al.*, 2019) in an interaction that depends on the
693 lipid composition of these membranes. The observation that fengycins are the major anti-fungal
694 factor produced by these strains *in vitro* and that these strains exhibit greater antagonism
695 towards the four mycoparasitic fungi, all of which belong to the order Hypocreales (Division:
696 Ascomycota) compared to *A. bisporus* (order Agaricales, Division Basidiomycota), raises the
697 prospect that this differential toxicity could relate to intrinsic differences in membrane
698 properties between fungi within these two clades. This suggests that biocontrol agents
699 specifically producing fengycins and selected or engineered to not produce broadly active anti-
700 fungal compounds could prove particularly effective as biocontrol agents for mushroom
701 cultivation. This also raises the exciting prospect that fengycins or other lipid-specific,
702 membrane-targeting compounds could be further developed as selective fungicides capable of
703 targeting specific groups of fungi. Research is already underway to develop approaches to
704 produce fengycin through fermentation on an industrial scale (Yin *et al.*, 2024). Additional
705 research could be carried out to determine which of the different analogues of fengycin
706 produced by *B. velezensis* and related bacteria display the greatest activity and specificity in
707 order to focus production on these metabolites.

708 Although fengycin remains the most likely candidate as the causal agent of the antimicrobial
709 activity observed *in vitro,* we have not yet been able to validate this hypothesis by knock-out
710 mutagenesis of the fengycin biosynthetic cluster, as the strains described in this study have
711 proven to be recalcitrant to transformation. However, the very low efficiency, but successful

712 transformation of CM19 with pHAPII gfp suggests that with further optimisation of
713 transformation protocols this might be possible. Additionally, we have not yet been able to
714 detect expression of fengycin biosynthetic genes or the production of fengycin when these
715 strains are inoculated into casing (data not shown), consistent with the rapid decline in
716 detectable bacteria and the lack of suppression of *L. fungicola* observed in crop trials.
717 Therefore, in order to fully realise the potential of fengycin-producing bacteria as biocontrol
718 agents it will be necessary to focus on the development of fengycins as selective fungicides or
719 further optimise the formulation and properties of these strains in the crop environment to
720 maximise survival and fengycin production.

721 **Conclusion**

722 In this study we set out to investigate whether endogenous casing bacteria have the potential to
723 be effective biocontrol agents against mycoparasitic fungi. *B. velezensis* strains isolated from
724 casing and basidiomes were demonstrated to display a high level of antifungal activity against
725 major fungal parasites, including *L. fungicola*, the causal agent of dry bubble. We identified a
726 fengycin analogue as the compound most likely to be responsible for the anti-fungal activity
727 exhibited by these strains *in vitro*. However, these strains have not been demonstrated to be
728 capable of suppressing the development of dry bubble when inoculated onto mushroom crops
729 that have been artificially infected with this parasite. The lack of antifungal activity observed
730 in crop could be due to a number of factors: the doses of mycoparasite and biocontrol agent
731 used, the level of fengycin present in or produced by the bacterial treatments applied to the
732 crop and the limited persistence of these strains in the casing material following inoculation.
733 In this sense, further optimisation of the bacteria formulation in relation to the composition and
734 dynamics of the microbiota that could compete for space or nutrients in the casing could be the

735 object of future research. Nevertheless, the specificity shown by these bacteria towards
736 mycoparasitic fungi over their mushroom host raises exciting possibilities to develop selective
737 biocontrol of mycoparasitic fungi. Understanding the composition and dynamics of the
738 microbiota in the casing during commercial cultivation of the fungus *A. bisporus* could be
739 essential to design novel biocontrol agents against mushroom mycoparasites.

740 **Tables**

741 Table 1: Experimental blocks used in crop trial

Treatment	**Code**	**Dose**	**Infected (*Lecanicillium fungicola* 150/1)**
Control	Control+	20 ml Tap water	10^6 conidia m^{-2} (10 days after casing)
Control	Control-	20 ml Tap water	-
Bacillus velezensis CM5	CM5	10^9 cfu* m^{-2}	10^6 conidia m^{-2} (10 days after casing)
Bacillus velezensis CM19	CM19	10^9 cfu m^{-2}	10^6 conidia m^{-2} (10 days after casing)
Bacillus velezensis CM35	CM35	10^9 cfu m^{-2}	10^6 conidia m^{-2} (10 days after casing)
Prochloraz-Mn	PCL	1 g m^{-2}	10^6 conidia m^{-2} (10 days after casing)

742 *cfu: colony forming unit.

743

Table 2: Summary of genomic data for *B. velezensis* casing isolates compared to QST713 (BLASTn (Nucleotide BLAST); BLASTp (Protein-Protein BLAST))**.**

	QST713	**CM5**	**CM19**	**CM35**	**EM5**	**EM39**
Similarity to [1]QST713 (%)	100	99.99	99.99	99.99	99.99	98.38
Genes (total)	4,238	4,256	4,255	4,256	4,256	3,906
GC Content	46	45.84	46	45.85	45.84	46.43
Genome Size	4233757	4240819	4240819	4240818	4240818	3929792
[2]CDSs (total)	4,047	4,137	4,136	4,137	4,137	3,788
Genes (coding)	4,047	4,049	4,048	4,048	4,048	3,686

CDSs (with protein)	4,047	4,049	4,048	4,048	4,048	3,686
Genes (RNA)	107	119	119	119	119	118
[3]rRNAs (5S, 16S, 23S)	9, 8, 8	10, 9, 9	10, 9, 9	10, 9, 9	10, 9, 9	9, 9, 9
Complete rRNAs (5S, 16S, 23S)	9, 8, 8	10, 9, 9	10, 9, 9	10, 9, 9	10, 9, 9	9, 9, 9
[4]tRNAs	77	86	86	86	86	86
[5]ncRNAs	5	5	5	5	5	5
Pseudo Genes (total)	84	88	88	89	89	102
CDSs (without protein)	84	88	88	89	89	102
Pseudo Genes (ambiguous residues)	0 of 84	0 of 88	0 of 88	0 of 89	0 of 89	0 of 102
Pseudo Genes (frameshifted)	48 of 84	51 of 88	51 of 88	52 of 89	52 of 89	61 of 102
Pseudo Genes (incomplete)	58 of 84	61 of 88	61 of 88	61 of 89	61 of 89	65 of 102
Pseudo Genes (internal stop)	14 of 84	11 of 88	11 of 88	11 of 89	11 of 89	9 of 102
Pseudo Genes (multiple problems)	30 of 84	29 of 88	29 of 88	29 of 89	29 of 89	30 of 102

744 [1]Results for all strains are from analyses using NCBI PGAAP (Tatusova *et al.*, 2016). Quality Assessment of
745 *Bacillus* genomes using QUAST can be found in Table S1; [2]CDS: Coding sequences; [3]rRNA: ribosomal RNA;
746 [4]tRNA: transfer RNA; [5]ncRNA: non-coding RNA.

747

748 Table 3: Comparative AntiSMASH analysis of gene clusters predicted to encode genes involved in
749 specialised metabolite synthesis between *Bacillus velezensis* CM5, CM19, CM35, EM5, EM39 and
750 QST713.

Most similar cluster	**Type**	**QST713**	**CM5**	**CM19**	**CM35**	**EM5**	**EM39**
bacillaene	Polyketide+[1]NRP	100%	100%	100%	100%	100%	100%
bacillibactin	NRP	100%	100%	100%	100%	100%	100%
bacilysin	Other	100%	100%	100%	100%	100%	100%
butirosin A/B	Saccharide	7%	7%	7%	7%	7%	7%
difficidin	Polyketide	100%	100%	100%	100%	100%	100%
fengycin	NRP	100%	100%	100%	100%	100%	100%
locillomycin	NRP+Polyketide	28%	28%	28%	28%	28%	-
macrolactin H	Polyketide	100%	100%	100%	100%	100%	100%
subtilin	[2]RiPP: Lanthipeptide	100%	100%	100%	100%	100%	-
surfactin	NRP:Lipopeptide	82%	82%	82%	82%	82%	82%

[1]NRP: Non-Ribosomal Peptides (built by non-ribosomal peptide synthetases (NRPSs)); [2]RiPPs: Ribosomally synthesized and Post-translationally modified Peptides.

Figures

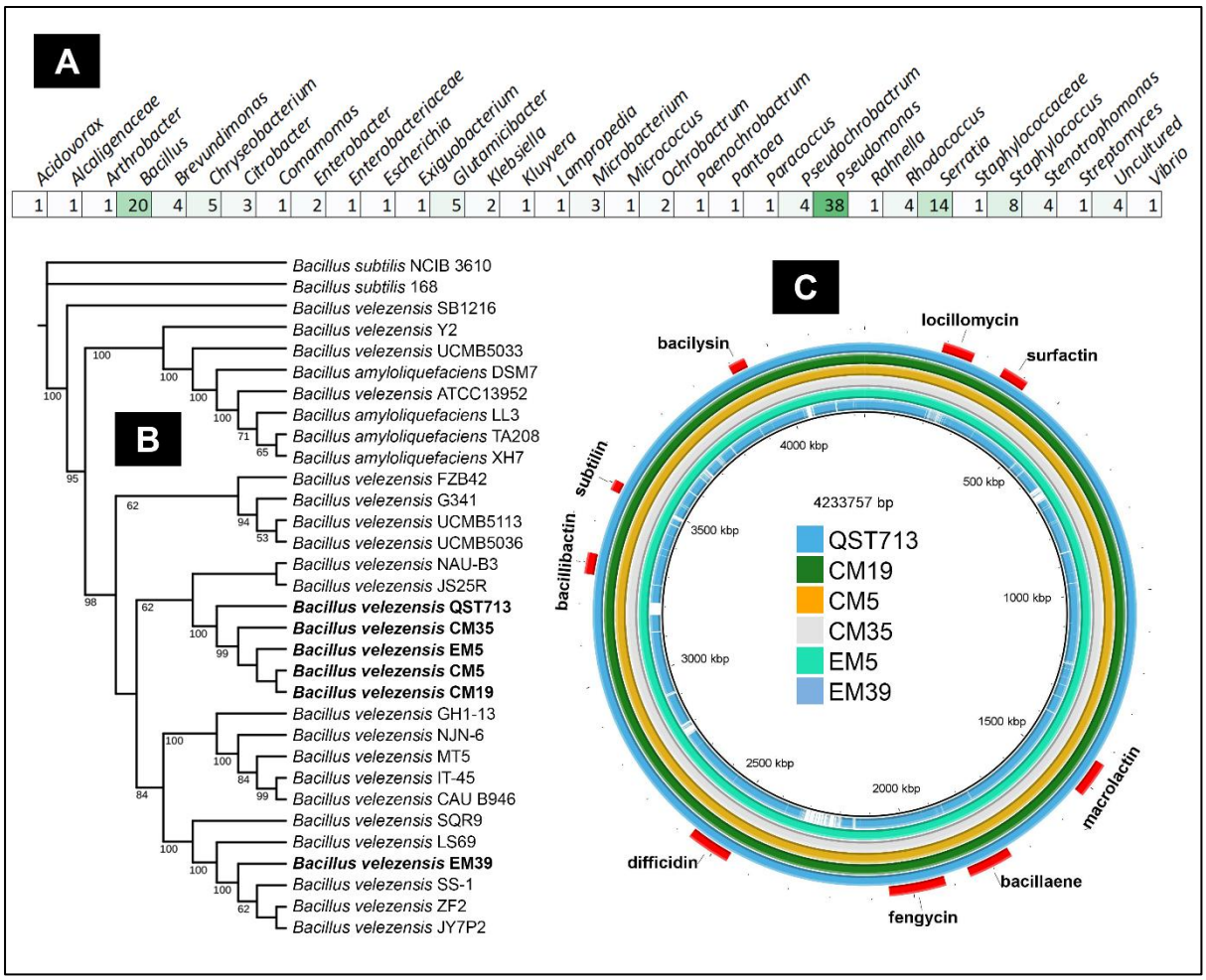

Figure 1: A) Cultivable bacterial isolates from three types of casing layer and endofungal bacteria from basidiomes of *Agaricus bisporus* identified using 16S rDNA sequencing; B) Phylogenetic tree of isolated *Bacillus* strains. The phylogeny was built using concatenated genomes comprising the five housekeeping genes (*gyrB*, *pgk*, *rpoB*, *rpoD*, and *tuf*) aligned to the reference strain *B. velezensis* FZB42. Strains highlighted in bold were isolated and phenotypically characterised in this study; C) Visualization of *Bacillus* genomes using circular map and BLAST comparison using BLAST Ring Generator (BRIG) (42); Putative specialised metabolite biosynthetic clusters compared to QST713 are shown by red marks in the outer ring.

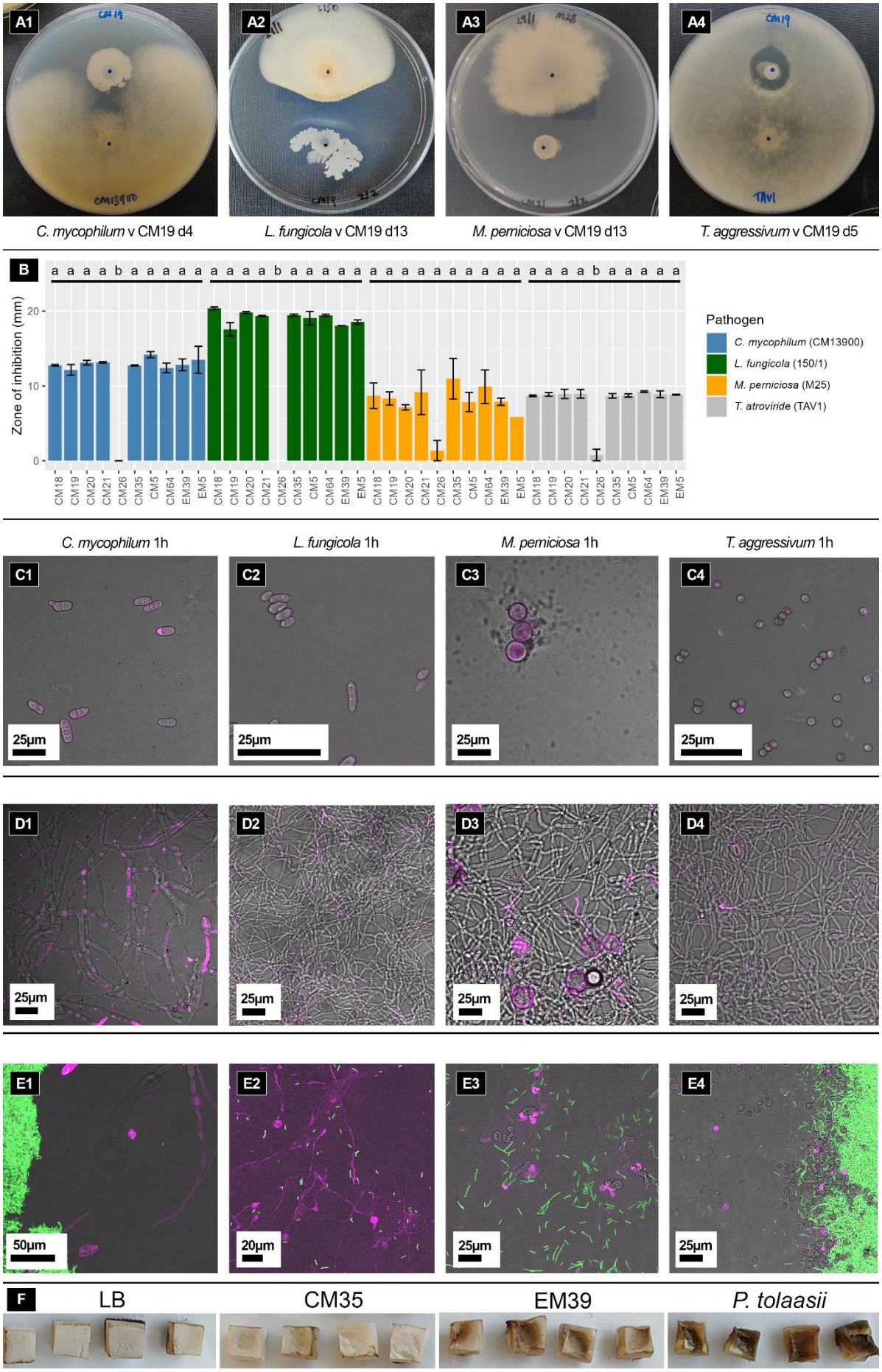
A1
A2
A3
A4
C. mycophilum v CM19 d4
L. fungicola v CM19 d13
M. perniciosa v CM19 d13
T. aggressivum v CM19 d5
B
Zone of inhibition (mm)
Pathogen
C. mycophilum (CM13900)
L. fungicola (150/1)
M. perniciosa (M25)
T. atroviride (TAV1)
C. mycophilum 1h
L. fungicola 1h
M. perniciosa 1h
T. aggressivum 1h
C1
C2
C3
C4
D1
D2
D3
D4
E1
E2
E3
E4
25µm
50µm
20µm
F
LB
CM35
EM39
P. tolaasii

763

764 Figure 2: A) Representative images of halos formed during antagonism between *B. velezensis* CM19
765 and the four fungal parasites of the cultivated button mushroom *Agaricus bisporus* in confrontation
766 assays: *L. fungicola* (150/1); *T. aggressivum* (TAV1); *M. perniciosa* (M25); and *C. mycophilum*
767 (CM13900). B) Graph shows the mean and standard error of zones of inhibition (mm) of the three
768 biological replicates of the antagonism assay. Letters indicate groups of statistically different conditions
769 (one-way ANOVA and Tukey's HSD test $\alpha = 0.05$). C & D) Representative images of unchallenged
770 fungal parasites grown *in vitro* on PDA plates – images taken using confocal microscope at t=0 (C),
771 and t=18 h (D). E) Representative confocal microscope images of fungal parasites *in vitro* in the
772 presence of *B. velezensis* CM19 transformed with the plasmid pHAPII gfp (green). Conidial and hyphal
773 viability and morphology were assessed *in vitro* using PDA plates. Live dead staining with propidium
774 iodide (PI; pink) was used to study the effect of CM19 on spore survival and germination (C, D, E).
775 Spores were classified as dead if either fully stained with PI or hollow/lysed cells. In many cases spores
776 were deemed to have germinated but resulting hyphae were also found to be stained or lysed. F)
777 Representative images of mushroom sporocarp cubes 24h after inoculation with LB, *B. velezensis*
778 CM35, *B. velezensis* EM39, and *P. tolaasii*. Graph of results can be viewed in Figure S1.

779

780

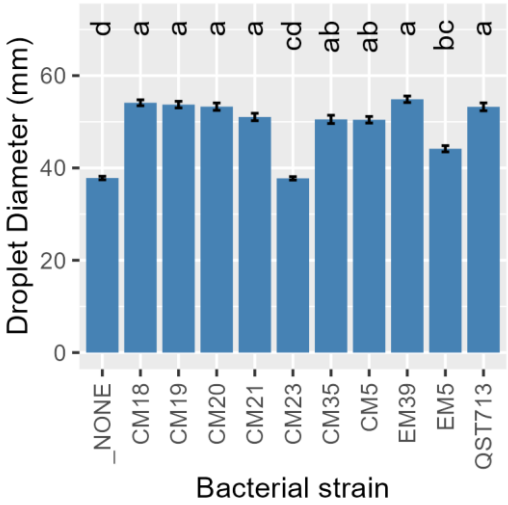

781

782 Figure 3: Surfactant production in *B. velezensis* strains. Data shown is the mean droplet diameter of
783 supernatant from overnight LB cultures. Droplet diameters were measured 2 minutes after pipetting
784 onto microscope slides. Graph shows the mean and standard error of 5 experiments, each containing 5
785 droplets per treatment. Letters indicate groups of statistically different conditions (one-way ANOVA
786 and Tukey's HSD test $\alpha = 0.05$).

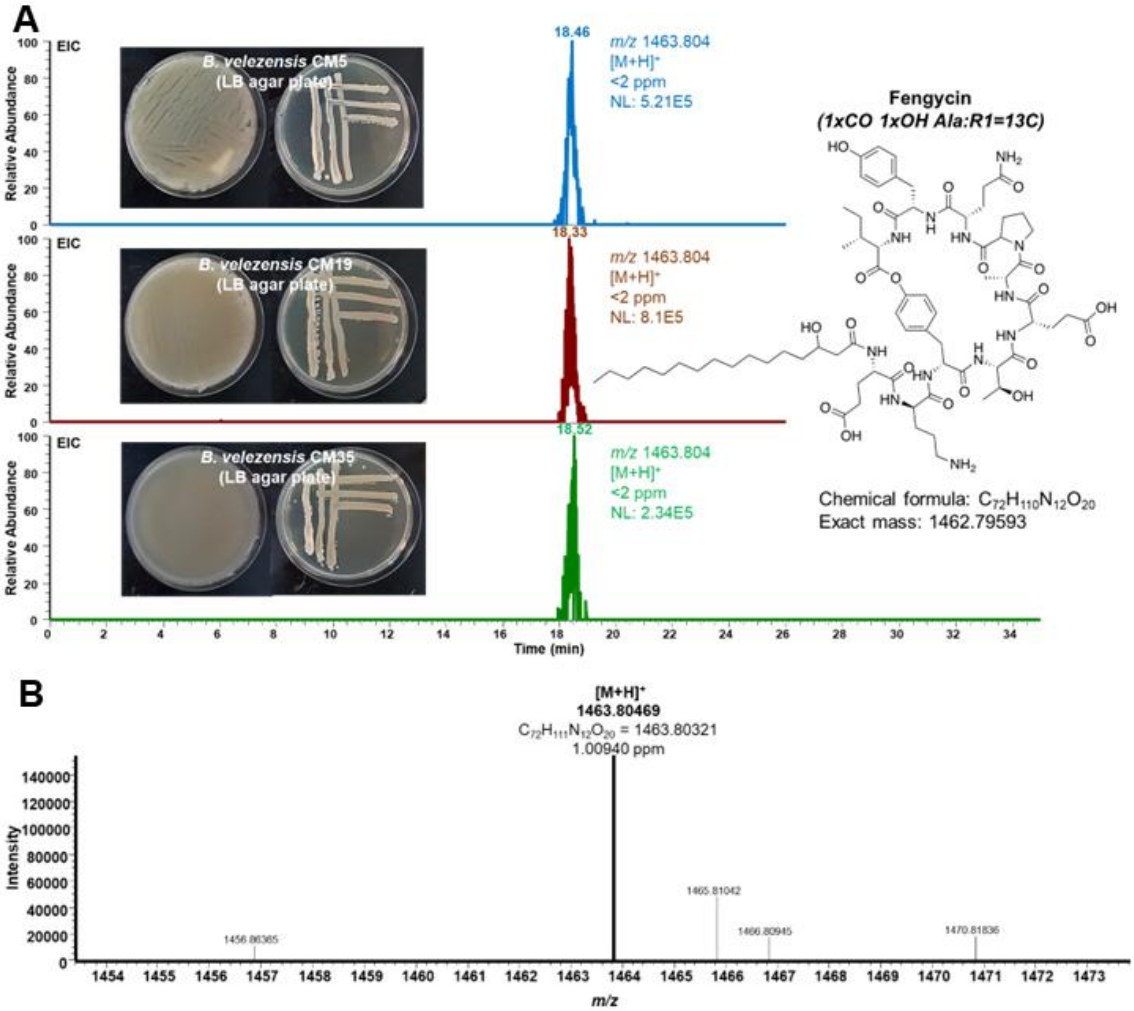

Figure 4: HPLC-HRMS analysis of fengycin produced by *B. velezensis* strains CM5, CM19 and CM35 cultivated on LB agar. (A) Extracted ion chromatograms ($[M+H]^+$, *m/z* 1463.804, ±2 ppm) show the production of fengycin by all the three strains. The highest physiological amounts of the compound were produced by *B. velezensis* CM19, followed by strains CM5 and CM35. The left insert shows the phenotypic characteristics of the strains grown on LB agar. The chemical structure of fengycin is shown on the right. (B) HRMS spectrum of fengycin produced by the bacteria.

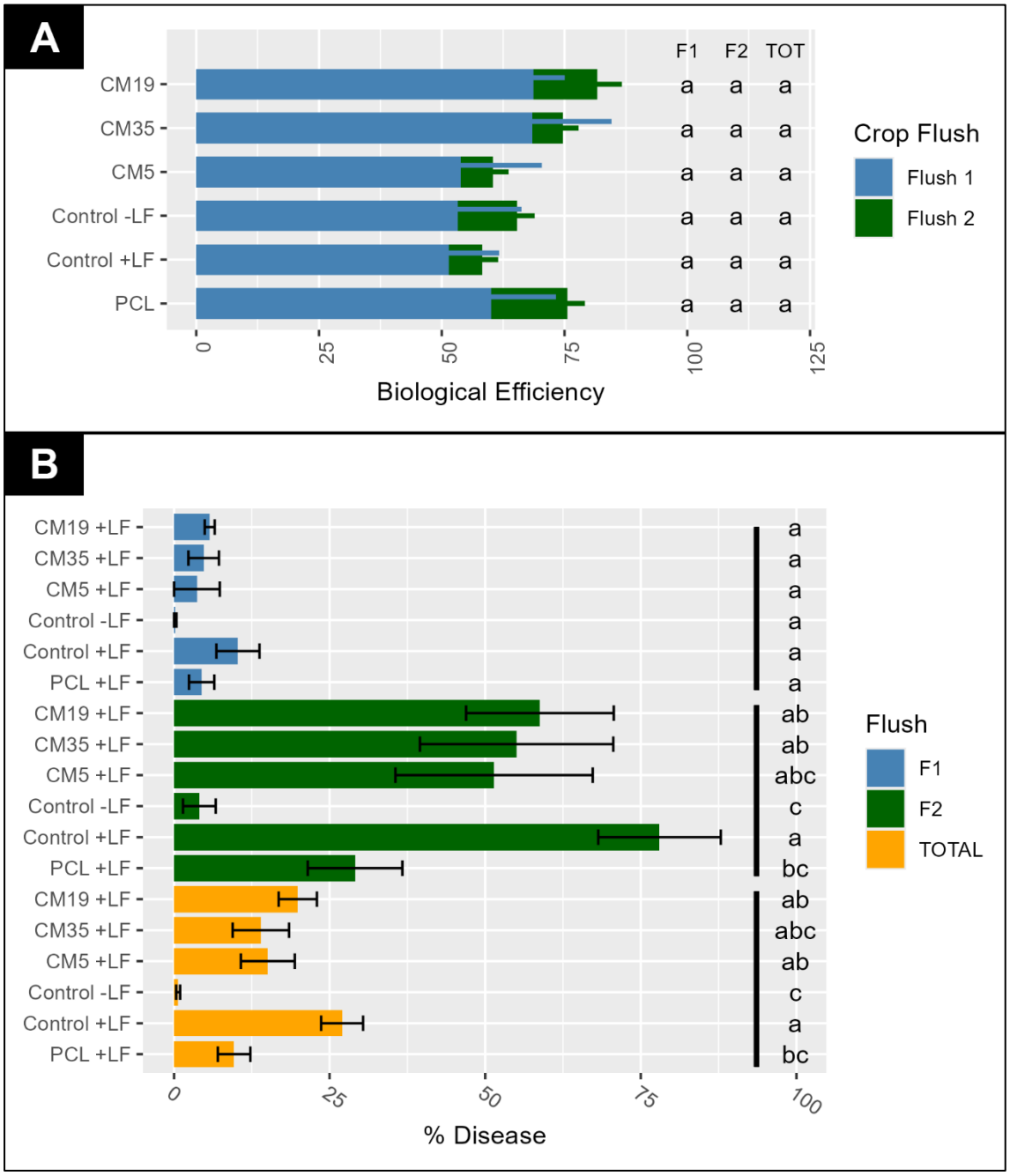

Figure 5: Crop trial of *B. velezensis* biocontrol activity against *Lecanicillium fungicola* 150/1. Blocks were artificially infected with *Lecanicillium fungicola* 150/1 and treated with CM5, CM19 and CM35, using prochloraz-Mn (PCL) as a positive control treatment and water as a negative control: A) Biological efficiency (BE) of the crop (Kg of mushroom per 100 Kg of compost in dry weight) recovered from the different treatments at flush 1 (F1), flush 2 (F2) and for the total cropping cycle; B) Diseased mushrooms (%) collected from the different treatments at F1, F2 and for the total cropping

803 cycle. Graphs show the mean and standard error of three biological replicates. Letters indicate groups

804 of statistically different conditions (one-way ANOVA and Tukey's HSD test $\alpha = 0.05$).

805

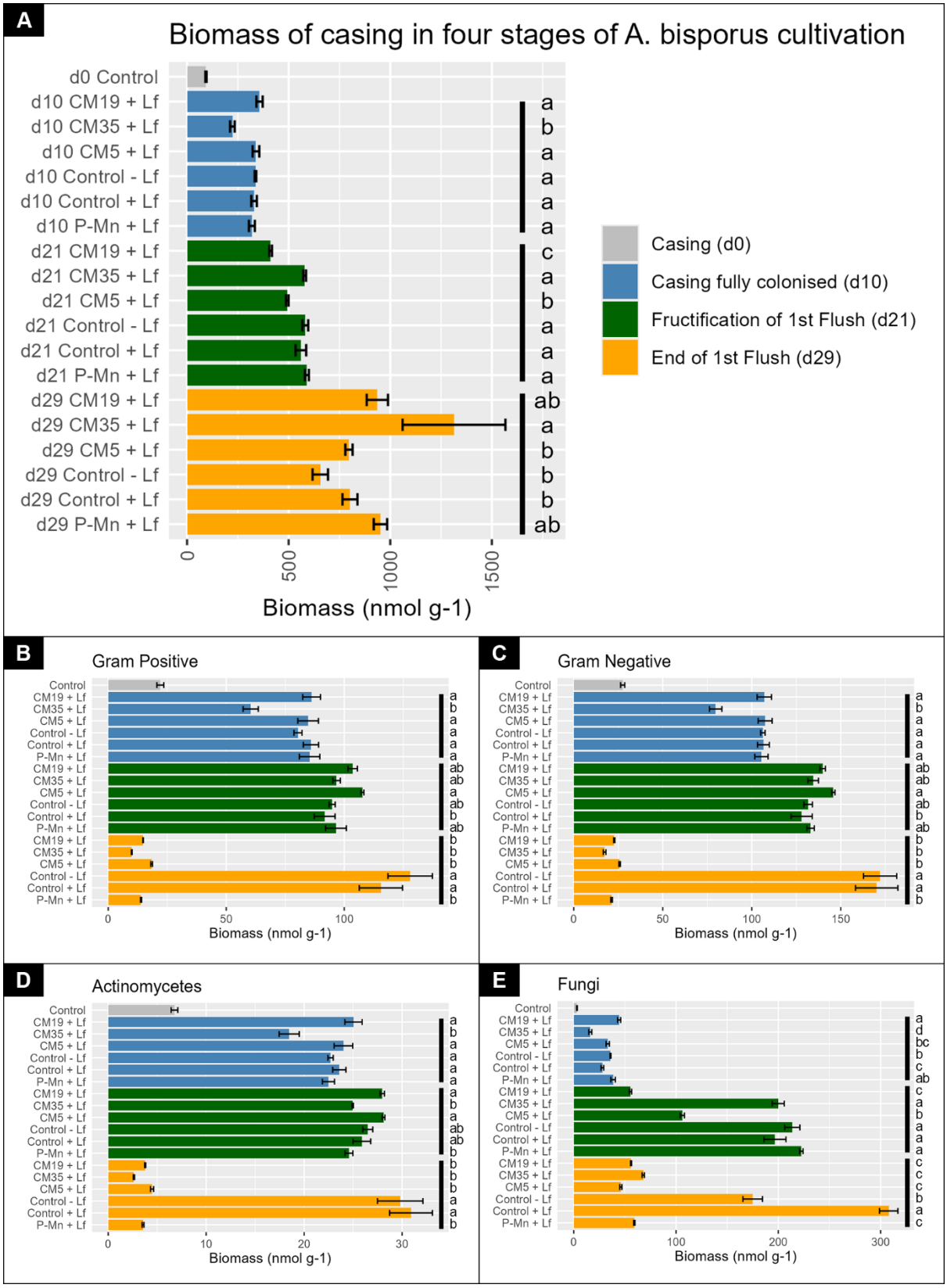

806

807 Figure 6: A: Quantification of casing microbial biomass by analysis of PLFAs. Four timepoints were

808 assessed: d0 (Beginning of trial; grey), day 10 (Fully colonized casing, blue), d21 (Fructification of first

flush, green), and d29 (End of first flush, orange). Treatment 1: Control +LF (+); Treatment 2: Control -LF (-); Treatment 3: CM5 +LF; Treatment 4: CM19 +LF; Treatment 5: CM35 +LF; Treatment 6: PCL +LF). Letters in uppercase highlight differences between treatments at the same time point (Tukey Test, $p > 0.05$). Error bars show SE. B: Abundance of Gram-positive bacteria. C: Abundance of Gram-negative bacteria. D: Abundance of Actinomycetes. E: Abundance of fungal PLFAs. All data shown uses nmol g-1.

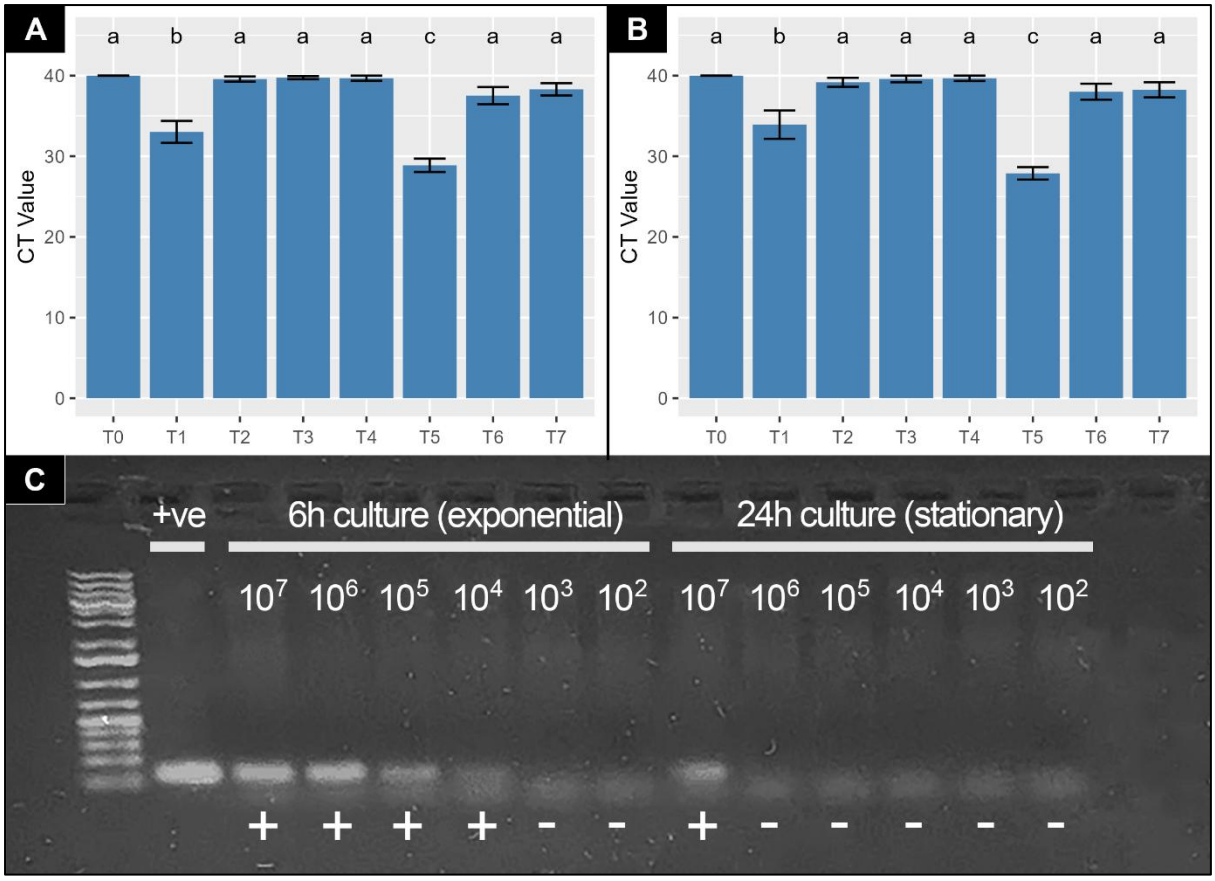

Figure 7: Population dynamics of *Bacillus velezensis* CM19 following application to mushroom casing as determined by a quantitative TaqMan assay. T0 = after cac-ing (day 0), T1 = directly after application of *B. velezensis* CM19 (day 3), T2 = End of spawn run (Day 9), T3 = Beginning of the 1st flush (Day 14), T4 = End of the 1st flush (Day 17), T5 = Directly after the second application of *B.velezensis* CM19 (Day 18), T6 = Beginning of the 2nd flush (Day 22), T7 = End of the 2nd flush (Day 25). A: Results using the HP2.21 (FAM) TaqMan probe; B) Results using the HP2.19 (Cy5) TaqMan probe C) Electrophoresis gel showing PCR results from PCR reaction using HP2.19 TaqMan primers (35 cycles) for DNA extracted from *B. velezensis* CM19 cells (from LB medium) in exponential growth stage (6h) and stationary cultures (24 h). Numbers indicate the number of bacteria added to the casing soil before extraction (cells added /g of soil).

Author statements

Authors

- William Kay; william.kay@biology.ox.ac.uk ; orcid.org/0000-0002-2561-4856
- Jaime Carrasco; jccarrasco@jccm.es; orcid.org/0000-0002-2051-1823 ,
- Gail Preston; gail.preston@biology.ox.ac.uk ; orcid.org/0000-0003-3882-4438
- Souvik Kusari: souvik.kusari@upjs.sk; orcid.org/0000-0002-4685-0794
- Marjon Krijger; Marjon.krijger@wur.nl
- M. José Carpio; mjose.carpio@ica.csic.es; orcid.org/0000-0003-1752-9608
- Thomas Barnes; tombarnes763@gmail.com
- M. Sonia Rodríguez Cruz; msonia.rodriguez@irnasa.csic.es; orcid.org/0000-0001-6748-3391
- Jan van der Woolf; jan.vanderwolf@wur.nl; orcid.org/0000-0002-9196-5419
- Till Bebenroth; till.bebenroth@tu-dortmund.de

Author Contributions

- *Conceptualization:* JC WK SK GP
- *Data curation:* WK JC SK MK MJC TB
- *Formal analysis:* JC MLT MT AT GP
- *Funding acquisition:* JC SK MSRC JVW GP
- *Investigation:* WK JC SK MK MJC TB MSRC JVW TB GP
- *Methodology:* WK JC SK MK MJC
- *Project administration:* JC SK MSRC JVW GP

- *Resources:* WK JC SK MK MJC TB MSRC JVW TB GP
- *Software:* WK JC SK MK MJC TB MSRC JVW TB GP
- *Supervision:* JC SK MSRC JVW GP
- *Validation:* WK JC SK MK MJC TB MSRC JVW TB GP
- *Visualization:* WK JC GP
- *Writing – original draft:* WK JC GP
- *Writing – review & editing:* WK JC SK MK MJC TB MSRC JVW TB GP

Conflicts of interest

There are no conflicts of interests. All the authors have read and approved the manuscript and all are aware of its submission to the Journal. The paper has not been submitted in any other journal.

Funding information

The project leading to this report has received funding from the European Union's Horizon 2020 research and innovation programme GA: 101000651 (BIOSCHAMP) and the Marie Sklodowska-Curie IF GA: 742966 (MYCOBIOME). JC is the recipient of a Ramon y Cajal contract [RYC2021-032796-I], funded by MCIN/AEI/10.13039/ 501100011033 and the European Union "NextGenerationEU"/PRTR".

Ethical approval

No ethics statement required since the work has been accomplished with commercial samples and wild strains from fungal specimens.

Acknowledgement

B. velezensis CM5, CM19 and CM35 are protected as biocontrol agents against mushroom parasites in a patent published as EP4200400A1; WO2021255181A1PCT. 2023/06/28. The project leading to this report has received funding from the European Union's Horizon 2020 research and innovation programme GA: 101000651 (BIOSCHAMP) and the Marie Sklodowska-Curie IF GA: 742966 (MYCOBIOME). JC is the recipient of a Ramon y Cajal contract [RYC2021-032796-I], funded by MCIN/AEI/10.13039/ 501100011033 and the European Union "NextGenerationEU"/PRTR".

References

1. Wang Q, Juan J, Xiao T, Zhang J, Chen H, Song X, et al. The physical structure of compost and C and N utilization during composting and mushroom growth in *Agaricus bisporus* cultivation with rice, wheat, and reed straw-based composts. Appl Microbiol Biotechnol. 2021;105:3811-23.

2. Dias ES, Zied DC, Pardo-Gimenez A. Revisiting the casing layer: Casing materials and management in *Agaricus* mushroom cultivation. Ciência e Agrotecnologia. 2021;45:e0001R21.

3. Fones HN, Bebber DP, Chaloner TM, Kay WT, Steinberg G, Gurr SJ. Threats to global food security from emerging fungal and oomycete crop pathogens. Nature Food. 2020;1(6):332-42.

4. Gea FJ, Navarro MJ, Santos M, Diánez F, Carrasco J. Control of fungal diseases in mushroom crops while dealing with fungicide resistance: a review. Microorganisms. 2021;9(3):585.

5. Sonnenberg AS, Baars JJ, Gao W, Visser RG. Developments in breeding of Agaricus bisporus var. bisporus: progress made and technical and legal hurdles to take. Appl Microbiol Biotechnol. 2017;101:1819-29.

6. Kosanović D, Potočnik I, Duduk B, Vukojević J, Stajić M, Rekanović E, et al. Trichoderma species on *Agaricus bisporus* farms in Serbia and their biocontrol. Annals of Applied Biology. 2013;163(2):218-30.

7. Commision E. Commission Implementing Regulation (EU) 2019/677 of 29 April 2019 concerning the non-renewal of the approval of the active substance chlorothalonil, in

accordance with Regulation (EC) No 1107/2009 of the European Parliament and of the Council concerning the placing of plant protection products on the market, and amending Commission Implementing Regulation (EU) No 40/2011. Official Journal of the European Union. 2019;114:15-7.

8. Zhang L, Sun C. Fengycins, cyclic lipopeptides from marine *Bacillus subtilis* strains, kill the plant-pathogenic fungus *Magnaporthe grisea* by inducing reactive oxygen species production and chromatin condensation. Applied Environmental Microbiology. 2018;84(18).

9. Carrasco J, Preston GM. Growing edible mushrooms: a conversation between bacteria and fungi. Environmental Microbiology. 2020;22(3):858-72.

10. Rabbee MF, Hwang B-S, Baek K-H. *Bacillus velezensis*: a beneficial biocontrol agent or facultative phytopathogen for sustainable agriculture. Agronomy. 2023;13(3):840.

11. Kenfaoui J, Dutilloy E, Benchlih S, Lahlali R, Ait-Barka E, Esmaeel Q. *Bacillus velezensis*: a versatile ally in the battle against phytopathogens—insights and prospects. Appl Microbiol Biotechnol. 2024;108(1):439.

12. Pandin C, Le Coq D, Deschamps J, Védie R, Rousseau T, Aymerich S, et al. Complete genome sequence of *Bacillus velezensis* QST713: A biocontrol agent that protects *Agaricus bisporus* crops against the green mould disease. Journal of Biotechnology. 2018;278:10-9.

13. Gao L, Guo J, Fan Y, Ma Z, Lu Z, Zhang C, et al. Module and individual domain deletions of NRPS to produce plipastatin derivatives in *Bacillus subtilis*. Microbial Cell Factories. 2018;17:1-13.

14. Desmyttere H, Deweer C, Muchembled J, Sahmer K, Jacquin J, Coutte F, et al. Antifungal activities of *Bacillus subtilis* lipopeptides to two *Venturia inaequalis* strains possessing different tebuconazole sensitivity. Frontiers in Microbiology. 2019;10:2327.

15. Zihalirwa Kulimushi P, Argüelles Arias A, Franzil L, Steels S, Ongena M. Stimulation of fengycin-type antifungal lipopeptides in *Bacillus amyloliquefaciens* in the presence of the maize fungal pathogen *Rhizomucor variabilis*. Frontiers in Microbiology. 2017;8:850.

16. Mantil E, Buznytska I, Daly G, Ianoul A, Avis TJ. Role of lipid composition in the interaction and activity of the antimicrobial compound fengycin with complex membrane models. The Journal of Membrane Biology. 2019;252:627-38.

17. Pandin C, Darsonval M, Mayeur C, Le Coq D, Aymerich S, Briandet R. Biofilm formation and synthesis of antimicrobial compounds by the biocontrol agent *Bacillus velezensis* QST713 in an *Agaricus bisporus* compost micromodel. Applied and Environmental Microbiology. 2019;85(12).

18. Kosanovic D, Dyas M, Grogan H, Kavanagh K. Differential proteomic response of Agaricus bisporus and *Trichoderma aggressivum* f. *europaeum* to *Bacillus velezensis* supernatant. European Journal of Plant Pathology. 2021;160(2):397-409.

19. Clarke J, Grogan H, Fitzpatrick D, Kavanagh K. Analysis of the effect of *Bacillus velezensis* culture filtrate on the growth and proteome of *Cladobotryum mycophilum*. Fungal Biology. 2022;126(1):11-9.

938 20. Clarke J, McGuinness B, Fitzpatrick D, Kavanagh K, Grogan H. Response of the
939 mushroom pathogen *Cladobotryum mycophilum* to the fungicides prochloraz and metrafenone
940 and two Bacillus-based biological control agents in mushroom crop trials. Crop Protection.
941 2024;177:106530.

942 21. Clarke J, Grogan H, Fitzpatrick D, Kavanagh K. Characterising the proteomic response
943 of mushroom pathogen *Lecanicillium fungicola* to *Bacillus velezensis* QST 713 and Kos
944 biocontrol agents. European Journal of Plant Pathology. 2022;163(2):369-79.

945 22. Novikova I, Titova J. Antifungal activity of Industrial *Bacillus* Strains against
946 *Mycogone perniciosa,* the causative agent of wet bubble disease in white button mushrooms.
947 Microorganisms. 2023;11(8):2056.

948 23. Steller S, Vollenbroich D, Leenders F, Stein T, Conrad B, Hofemeister J, et al.
949 Structural and functional organization of the fengycin synthetase multienzyme system from
950 *Bacillus subtilis* b213 and A1/3. Chemistry & Biology. 1999;6(1):31-41.

951 24. Yin Y, Wang X, Zhang P, Wang P, Wen J. Strategies for improving fengycin
952 production: a review. Microbial Cell Factories. 2024;23(1):144.

953 25. Sang-Cheol L, Kim S-H, Park I-H, Chung S-Y, Chandra MS, Yong-Lark C. Isolation,
954 purification, and characterization of novel fengycin S from *Bacillus amyloliquefaciens* LSC04
955 degrading-crude oil. Biotechnology and Bioprocess Engineering. 2010;15:246-53.

956 26. Villegas-Escobar V, Ceballos I, Mira JJ, Argel LE, Orduz Peralta S, Romero-Tabarez
957 M. Fengycin C produced by *Bacillus subtilis* EA-CB0015. Journal of Natural Products.
958 2013;76(4):503-9.

959 27. Kalamara M, Spacapan M, Mandic-Mulec I, Stanley-Wall NR. Social behaviours by
960 *Bacillus subtilis*: quorum sensing, kin discrimination and beyond. Mol Microbiol.
961 2018;110(6):863-78.

962 28. Na H-E, Heo S, Kim T, Lee G, Lee J-H, Jeong D-W. ComQXPA quorum-sensing
963 systems contribute to enhancing the protease activity of Bacillus velezensis DMB05 from
964 fermented soybeans. International Journal of Food Microbiology. 2023;401:110294.

965 29. Carrasco J, Tello ML, de Toro M, Tkacz A, Poole P, Pérez-Clavijo M, et al. Casing
966 microbiome dynamics during button mushroom cultivation: implications for dry and wet
967 bubble diseases. Microbiology. 2019;165(6):611-24.

968 30. Aslani MA, Harighi B, Abdollahzadeh J. Screening of endofungal bacteria isolated
969 from wild growing mushrooms as potential biological control agents against brown blotch and
970 internal stipe necrosis diseases of *Agaricus bisporus*. Biological Control. 2018;119:20-6.

971 31. Stackebrandt E, Goodfellow M. Nucleic acid techniques in bacterial systematics.
972 Wiley, editor. Chichester ; New York: Wiley; 1991. xxix,329p. p.

973 32. Camacho C, Coulouris G, Avagyan V, Ma N, Papadopoulos J, Bealer K, et al. BLAST+:
974 architecture and applications. BMC Bioinformatics. 2009;10:1-9.

975 33. Bolger AM, Lohse M, Usadel B. Trimmomatic: a flexible trimmer for Illumina
976 sequence data. Bioinformatics. 2014;30(15):2114-20.

977 34. Bankevich A, Nurk S, Antipov D, Gurevich AA, Dvorkin M, Kulikov AS, et al.
978 SPAdes: a new genome assembly algorithm and its applications to single-cell sequencing.
979 Journal of Computational Biology. 2012;19(5):455-77.

980 35. Seemann T. Prokka: rapid prokaryotic genome annotation. Bioinformatics.
981 2014;30(14):2068-9.

982 36. Rutherford K, Parkhill J, Crook J, Horsnell T, Rice P, Rajandream M-A, et al. Artemis:
983 sequence visualization and annotation. Bioinformatics. 2000;16(10):944-5.

984 37. Gurevich A, Saveliev V, Vyahhi N, Tesler G. QUAST: quality assessment tool for
985 genome assemblies. Bioinformatics. 2013;29(8):1072-5.

986 38. Wood DE, Salzberg SL. Kraken: ultrafast metagenomic sequence classification using
987 exact alignments. Genome biology. 2014;15(3):1-12.

988 39. Aziz RK, Bartels D, Best AA, DeJongh M, Disz T, Edwards RA, et al. The RAST
989 Server: rapid annotations using subsystems technology. BMC Genomics. 2008;9(1):1-15.

990 40. Aziz RK, Devoid S, Disz T, Edwards RA, Henry CS, Olsen GJ, et al. SEED servers:
991 high-performance access to the SEED genomes, annotations, and metabolic models. PloS one.
992 2012;7(10):e48053.

993 41. Tatusova T, DiCuccio M, Badretdin A, Chetvernin V, Nawrocki EP, Zaslavsky L, et al.
994 NCBI prokaryotic genome annotation pipeline. Nucleic Acids Research. 2016;44(14):6614-24.

995 42. Alikhan N-F, Petty NK, Ben Zakour NL, Beatson SA. BLAST Ring Image Generator
996 (BRIG): simple prokaryote genome comparisons. BMC Genomics. 2011;12(1):402.

997 43. Blin K, Shaw S, Kloosterman AM, Charlop-Powers Z, Van Wezel GP, Medema MH,
998 et al. antiSMASH 6.0: improving cluster detection and comparison capabilities. Nucleic Acids
999 Research. 2021;49(W1):W29-W35.

1000 44. Edgar RC. MUSCLE: multiple sequence alignment with high accuracy and high
1001 throughput. Nucleic Acids Research. 2004;32(5):1792-7.

1002 45. Nguyen L-T, Schmidt HA, Von Haeseler A, Minh BQ. IQ-TREE: a fast and effective
1003 stochastic algorithm for estimating maximum-likelihood phylogenies. Molecular Biology and
1004 Evolution. 2015;32(1):268-74.

1005 46. Letunic I, Bork P. Interactive Tree Of Life (iTOL) v5: an online tool for phylogenetic
1006 tree display and annotation. Nucleic Acids Research. 2021;49(W1):W293-W6.

1007 47. Cao Y, Zhang Z, Ling N, Yuan Y, Zheng X, Shen B, et al. *Bacillus subtilis* SQR 9 can
1008 control Fusarium wilt in cucumber by colonizing plant roots. Biology and Fertility of Soils.
1009 2011;47:495-506.

1010 48. Morales-Ruiz E, López-Ceballos A, Maldonado-Mendoza IE. Transformation of the
1011 rhizospheric *Bacillus cereus* sensu lato B25 strain using a room-temperature electrocompetent
1012 cells preparation protocol. Plasmid. 2019;105:102435.

1013 49. Banks AM, Aminuddin F, Williams K, Batstone T, Barker GL, Foster GD, et al.
1014 Genome sequence of *Lecanicillium fungicola* 150-1, the causal agent of dry bubble disease.
1015 Microbiology Resource Announcements. 2019;8(19):10.1128/mra. 00340-19.

1016 50. Gea FJ, Carrasco J, Diánez F, Santos M, Navarro MJ. Control of dry bubble disease
1017 (*Lecanicillium fungicola*) in button mushroom (*Agaricus bisporus*) by spent mushroom
1018 substrate tea. European Journal of Plant Pathology. 2014;138:711-20.

1019 51. Frostegård Å, Tunlid A, Bååth E. Phospholipid fatty acid composition, biomass, and
1020 activity of microbial communities from two soil types experimentally exposed to different
1021 heavy metals. Applied and Environmental Microbiology. 1993;59(11):3605-17.

1022 52. Zelles L. Fatty acid patterns of phospholipids and lipopolysaccharides in the
1023 characterisation of microbial communities in soil: a review. Biology and Fertility of Soils.
1024 1999;29:111-29.

1025 53. Hammer O, Harper DA, Ryan PD. Palaeontological statistics software package for
1026 education and data analysis. Palaeontologia Electronica. 2001;4(1):1-9.

1027 54. Taparia T, Krijger M, Hodgetts J, Hendriks M, Elphinstone JG, Van der Wolf J. Six
1028 multiplex TaqManTM-qPCR assays for quantitative diagnostics of pseudomonas species
1029 causative of bacterial blotch diseases of mushrooms. Frontiers in Microbiology. 2020;11:989.

1030 55. Köhl J, Vlaswinkel M, Groenenboom-de Haas B, Kastelein P, Van Hoof R, Van der
1031 Wolf J, et al. Survival of pathogens of Brussels sprouts (*Brassica oleracea* Gemmifera Group)
1032 in crop residues. Plant Pathology. 2011;60(4):661-70.

1033 56. Pandin C, Le Coq D, Canette A, Aymerich S, Briandet R. Should the biofilm mode of
1034 life be taken into consideration for microbial biocontrol agents? Microbial Biotechnology.
1035 2017;10(4):719-34.

1036 57. Godfrey S, Harrow S, Marshall J, Klena J. Characterization by 16S rRNA sequence
1037 analysis of pseudomonads causing blotch disease of cultivated *Agaricus bisporus*. Applied and
1038 Environmental Microbiology. 2001;67(9):4316-23.

1039 58. Fan B, Blom J, Klenk H-P, Borriss R. *Bacillus amyloliquefaciens*, *Bacillus velezensis*,
1040 and *Bacillus siamensis* form an "operational group *B. amyloliquefaciens*" within the *B. subtilis*
1041 species complex. Frontiers in Microbiology. 2017;8:237721.

1042 59. Sur, S, Romo, TD, Grossfield, A. Selectivity and mechanism of fengycin, an
1043 antimicrobial lipopeptide, from molecular dynamics. The Journal of Physical Chemistry B.
1044 2018;122(8):2219-2226.

1045 60. Gilliard, G, Demortier, T, Boubsi, F, Jijakli, MH, Ongena, M, De Clerck, C, Deleu, M.
1046 Deciphering the distinct biocontrol activities of lipopeptides fengycin and surfactin through
1047 their differential impact on lipid membranes. Colloids and Surfaces B: Biointerfaces.
1048 2024;239:113933.

1049 61. Qin, Y, He, Y, She, Q, Larese-Casanova, P, Li, P, Chai, Y. Heterogeneity in respiratory
1050 electron transfer and adaptive iron utilization in a bacterial biofilm. Nature Communications.
1051 2019;10(1):3702.

1052 62. Akpa E, Jacques P, Wathelet B, Paquot M, Fuchs R, Budzikiewicz H, et al. Influence
1053 of culture conditions on lipopeptide production by *Bacillus subtilis*. Applied Biochemistry and
1054 Biotechnology. 2001;91(1):551-61.

1055 63. Wang J, Liu J, Wang X, Yao J, Yu Z. Application of electrospray ionization mass
1056 spectrometry in rapid typing of fengycin homologues produced by *Bacillus subtilis*. Letters in
1057 Applied Microbiology. 2004;39(1):98-102.

1058 64. Ma Y, Kong Q, Qin C, Chen Y, Chen Y, Lv R, et al. Identification of lipopeptides in
1059 *Bacillus megaterium* by two-step ultrafiltration and LC–ESI–MS/MS. Amb Express. 2016;6:1-
1060 15.

1061 65. Carrasco J, Zied DC, Navarro MJ, Gea FJ, Pardo-Giménez A. Commercial cultivation
1062 techniques of mushrooms. Advances in Macrofungi: CRC Press; 2021. p. 11-40.

1063 66. Braat N, Koster MC, Wösten HA. Beneficial interactions between bacteria and edible
1064 mushrooms. Fungal Biology Reviews. 2022;39:60-72.

1065 67. Carrasco J, Preston G, inventors; Asociación Profesional De Productores De Sustratos
1066 Y Hongos De La Rioja, Navarra Y Aragón, assignee. Bacteria2023.

1067 68. Anastassiadou M, Arena M, Auteri D, Brancato A, Bura L, Carrasco Cabrera L, et al.
1068 Peer review of the pesticide risk assessment of the active substance *Bacillus amyloliquefaciens*
1069 strain QST 713 (formerly *Bacillus subtilis* strain QST 713). EFSA Journal. 2021;19(1):e06381.

1070 69. Navarro MJ, Santos M, Diánez F, Gea FJ. Chemical and biological control of wet
1071 bubble disease (*Hypomyces perniciosus*) in mushroom crops. Agronomy. 2023;13(7):1672.

1072 70. Carrasco J, García-Delgado C, Lavega R, Tello ML, De Toro M, Barba-Vicente V, et
1073 al. Holistic assessment of the microbiome dynamics in the substrates used for commercial
1074 champignon (*Agaricus bisporus*) cultivation. Microbial Biotechnology. 2020;13(6):1933-47.

1075 71. Wei-Ming C, Huai-Ying Y, Wei-Lin F, Qun-Li J, Yue-Yan L, Nan-Yi L, et al.
1076 Microbial community structure of casing soil during mushroom growth. Pedosphere.
1077 2009;19(4):446-52.

1078 72. Zhao Y, Li T, Shao P, Sun J, Xu W, Zhang Z. Variation in bacterial community
1079 structure in rhizosphere and bulk soils of different halophytes in the yellow river delta.
1080 Frontiers in Ecology and Evolution. 2022;9:816918.

1081 73. Rainey PB. The involvement of *Pseudomonas putida* in basidiome initiation of the
1082 cultivated mushroom Agaricus bisporus. 1989.

1083 74. Noble R, Fermor TR, Lincoln S, Dobrovin-Pennington A, Evered C, Mead A, et al.
1084 Primordia initiation of mushroom (*Agaricus bisporus*) strains on axenic casing materials.
1085 Mycologia. 2003;95(4):620-9.

1086 75. Lacey J. Actinomycetes in compost. Annals of Agricultural and Environmental
1087 Medicine. 1997;4(1).

1088 76. Akond MA, Jahan MN, Sultana N, Rahman F. Effect of temperature, pH and NaCl on
1089 the isolates of actinomycetes from straw and compost samples from Savar, Dhaka, Bangladesh.
1090 American Journal of Microbiology and Immunology. 2016;1(2):10-5.

1091 77. Ochi K. Insights into microbial cryptic gene activation and strain improvement:
1092 principle, application and technical aspects. The Journal of Antibiotics. 2017;70(1):25-40.

1093 78. Zakharova AA, Efimova SS, Malev VV, Ostroumova OS. Fengycin induces ion
1094 channels in lipid bilayers mimicking target fungal cell membranes. Scientific Reports.
1095 2019;9(1):16034.

1096

1097